HYDRODYNAMICS AND HEAT TRANSFER IN UPWARD INCLINED GAS-LIQUID TWO-PHASE TWO-COMPONENT FLOWS

By

RANGA NANDA KISHORE KORIVI

Bachelor of Technology in Mechanical Engineering

Jawaharlal Nehru Technological University

Kakinada, India

2013

Submitted to the Faculty of the
Graduate College of the
Oklahoma State University
in partial fulfillment of
the requirements for
the Degree of
MASTER OF SCIENCE
December, 2015

HYDRODYNAMICS AND HEAT TRANSFER IN

UPWARD INCLINED GAS-LIQUID TWO-PHASE

TWO-COMPONENT FLOWS

Thesis Approved:

Dr. Afshin Ghajar

Thesis Adviser

Dr. Khaled A. Sallam

Dr. AJ Johannes

ACKNOWLEDGEMENTS

Firstly, I would like to express most profound gratitude to my advisor, Dr. Afshin J. Ghajar for his consistent guidance and immense support. It might have been impossible to withstand all the past difficulties without his support. I would also like to convey my most sincere thanks to my committee members Dr. Khaled A. Sallam and Dr. AJ Johannes for their amiability, support and helpful comments.

I would also like to thank Swanand Bhagwat for his consistent support and valuable guidance throughout this study. This process is not complete without thanking Srinaga Kalapatapu, Tabassum Hossainy and Edgar Barboza for providing enormous support with getting the research started. A special thanks is due to my lab partner Tarebi J. John, who was an excellent team member and a good friend.

Finally, I would like to thank my family for their endless love and support. A very special thanks is due to my mother, sister and grandmother for their unwavering moral support. This work is dedicated to my late grandfather, Sambasiva Rao. Kotapati. He is my role model and inspiration.

Name: RANGA NANDA KISHORE KORIVI

Date of Degree: DECEMBER, 2015

Title of Study: HYDRODYNAMICS AND HEAT TRANSFER IN UPWARD INCLINED GAS-LIQUID TWO-PHASE TWO-COMPONENT FLOWS

Major Field: MECHANICAL AND AEROSPACE ENGINEERING

Abstract: Two-phase two-component heat transfer in gas-liquid two phase flows embraces some of the practical applications pertinent to chemical industry and oil and gas industry. In comparison to horizontal and vertical two phase flows, very little information is available about non-boiling heat transfer in upward pipe inclinations. To further understand this phenomenon, 617 experimental measurements of the local and space averaged two phase heat transfer coefficients are carried out in 0^0, $+5^0$, $+10^0$, $+15^0$, $+20^0$, $+30^0$, $+45^0$, $+60^0$, $+75^0$ and $+90^0$ degrees of pipe inclinations using air-water fluid combination in a 12.5 mm I.D. stainless steel pipe. The measured non-boiling two phase heat transfer coefficients are found to be influenced by phase flow rates, pipe orientation, flow patterns, fluid combinations and pipe diameters. The two phase heat transfer coefficient is observed to increase with increasing pipe orientation from horizontal to the vicinity of $+60^0$ to $+75^0$ and then shows a decreasing trend or tends to stay constant as the pipe is inclined towards vertical position depending on the liquid flow rate. The effect of change in flow pattern structure on the measured two heat transfer coefficient is noticeable for bubbly and slug flows compared to that in intermittent and annular flow patterns. The heat transfer coefficient in two phase flow is found to be much greater than that in single phase flow. The experimental data comprising of 617 data points from the present study and 718 data points procured from the literature to include various fluid combinations and pipe diameters are used to scrutinize the performance of some of the widely accepted two phase heat transfer correlations available in the literature. Based on a statistical performance, the top performing correlations for different flow patterns, pipe orientations, fluid combinations and pipe diameters are recommended.

TABLE OF CONTENTS

LIST OF TABLES

Table Page

LIST OF FIGURES

Figure Page

NOMENCLACURE

A	cross sectional area, m^2
c	specific heat capacity, kJ/kg.K
D_i	inside diameter of pipe, m
D_o	outside diameter of pipe, m
f	function operator, dimensionless
F_p	flow pattern factor, dimensionless
F_s	shape factor, dimensionless
G	mass flux, kg/m²s
Gr	Grashof number, dimensionless
g	gravitational acceleration, m/s^2
I	electric current, A or inclination factor, dimensionless from Tang and Ghajar (2007)
h	heat transfer coefficient, W/m².K
$\bar{h}$	local average heat transfer coefficient, W/m².K
j	flow rate, m^3/s
J	mass flow rate, kg/hr
k	thermal conductivity, W/m.K

K	slip ratio, dimensionless
l	length of test section, m
$\dot{m}$	mass flow rate, kg/s
Nu	Nusselt number (= hD_i/k), dimensionless
N	number of data points, dimensionless
N_{ST}	number of thermocouple stations, dimensionless
Pr	Prandtl number (= $c\mu/k$), dimensionless
p	pressure, Pa
p_a	atmospheric pressure, Pa
p_{sys}	system pressure, Pa
$\dot{q}$	heat transfer rate, W
$\dot{q}''$	heat flux, W/m^2
R	electrical resistance, Ω
R_L	liquid hold up, dimensionless
R_t	thermal resistance, m^{2}K/W
R_v	gas to liquid volumetric ratio, dimensionless
Re	Reynolds number (= $\rho VD_i/\mu$), dimensionless
T	temperature, ^{o}C
$\bar{T}$	average temperature, ^{o}C

V average velocity, m/s

V_D voltage drop, V

w uncertainty, dimension varies with measured parameter

x flow quality $\dot{m}_G/\dot{m}$, dimensionless

x_n independent variable, dimension varies with variable

z axial direction, m

Greek Symbols

α void fraction, dimensionless

Δ differential operator, dimensionless

ε error, dimensionless

$\bar{\varepsilon}$ mean error, dimensionless

μ dynamic viscosity, N.m/s^2

ν kinematic viscosity, m^2/s

ρ density, kg/m^3

σ surface tension, N/m

θ inclination angle of pipe or test section, deg. or rad.

Subscripts

b bulk

cal calculated

exp experimental

G gas phase

H homogeneous mixture

in inlet

j index in the circumferential direction, or *j*th component of data set

L liquid phase

m mixture

n number of variable

out outlet

SG superficial gas

SL superficial liquid

TP two phase

w wall

wi inner wall

wo outer wall

Superscripts

p constant exponent, dimensionless

CHAPTER I

INTRODUCTION

A phase is defined as a state of matter with identifiable class of materials. A two-phase flow involves simultaneous movement of any two out of the three phases (solid, liquid and gas). These two-phase flows can be broadly classified as one-component and two-component two-phase flows. The one-component two-phase flow is caused by the phase change process and consist of different phases of same substance such as steam-water flows, generally seen in power plants, nuclear plants, refrigeration plants and air conditioning plants. On the other hand a two-component two-phase flow involve a flow of two immiscible phase of chemically different substances like air-water flows. These two-component two-phase flows are predominantly seen in oil and natural gas industry, process industry and also in chemical industry. The prime scope of this work is to study the two-component two-phase flows with gas-liquid combinations, due to their wide spread applications. The behavior of the two-phase two-component flows differ from the single phase flows due to the additional interface interactions providing a major obstacle in computing a theoretical solution. For computing a theoretical solution to two-phase flows, it is necessary to solve the Navier-Stokes equations for each particle in both phases and at the characteristic interface separating them. Hence, experimental approach is preferred due to this demand of astronomical computational power by the theoretical solutions.

The two-phase two-component flow finds its applications in a wide range of industrial processes and it is essential to accurately estimate the flow structure and heat transfer phenomenon of these flows for optimized design, safe performance, prediction of operational limits and to diagnose faults in less fortunate situations. In oil and natural gas industry the hydrocarbon fluids are transported in pipelines and wellbores. Generally these hydrocarbon fluids are at a higher temperature than the pipelines and wellbores, due to this temperature difference between the wall and the fluid combination there is a heat transfer between them. This allows for the formation of gas hydrate and wax deposition blockages in the pipe, which cause severe production and functioning problems to the plant due to the reduction in the pipe diameter and also by the increase in the surface roughness of the pipe surface as analyzed by McClaflin and Whitfill (1984). These problems can often result in huge economic losses like the 100 million dollars incurred by Lasmo Company in U.K for abandoning an oil platform (Singh et al., 2000). In certain situations increased heat transfer in reduced space is desired like those seen in heat exchangers, refrigerators and space craft designs. Two-phase flows are a very effective way to achieve this increase in heat transfer apart from other convectional techniques of promoting turbulence like increasing surface roughness, inserting helical ribs and coiled springs.

Celata et al. (1999) proved that two phase flows can also be used to increase the heat transfer coefficient by studying water flows with and without air injections in a uniformly heated vertical pipe. They observed a 20-40% increase in the heat transfer coefficient for forced-convection and even larger growth in mixed-convection. Many industrial applications involve transportation of two-phase through long distances, where it is very difficult to know the exact flow patterns and also it is inevitable to encounter pipe inclinations in these cases. A typical situation of this type is seen in oil and natural gas industry, where long pipe lines are used to connect the remote oil wells to the processing stations. Thus, it is very important to have an idea on effect of pipe inclinations on two-phase flows and to develop a predictive method to compute the heat transfer irrespective

of flow pattern. It is also not unusual to employ pipes of different diameters to transfer different fluid combinations depending on the discharge required at the receiving facility, which is generally seen in chemical industries. So, it also of interest to identify a model that can predict the heat transfer phenomenon irrespective of fluid combinations used and pipe diameters.

1.1 Definitions and Terminologies

In this section, an overview of terminologies used to describe two phase flow is presented. Two-phase flows depends on several factors like nature of the gas, nature of liquid and pipe dimensions and are more complicated than the single phase flow due to additional interface interactions. So, additional terms are provided to explain the behavior of the two-phase flows mathematically. The definitions presented here are for one dimensional flows in a pipe, which is relevant to the present work.

Two phase mass flow rate is the summation of the gas mass flow rate and liquid mass flow rate.

$$\dot{m} = \dot{m}_G + \dot{m}_L \tag{1.1}$$

The definition of liquid, gas and mixture mass flux are commonly defined as:

$$G_G = \frac{\dot{m}_G}{A} \tag{1.2a}$$

$$G_L = \frac{\dot{m}_L}{A} \tag{1.2b}$$

$$G = \frac{\dot{m}}{A} \tag{1.2c}$$

Where, the cross sectional area is the summation of the cross sectional area occupied by both the liquid and gas phase.

$$A = A_G + A_L \tag{1.3}$$

The quality of the flow shows the ratio of mass flux of gas to that of the total mass flow rate of the mixture as given below

$$x = \frac{\dot{m}_G}{\dot{m}} \tag{1.4}$$

The void fraction (α) is the defined as the area of space the gas phase occupies to the total cross sectional area as shown below.

$$\alpha = \frac{A_G}{A} \tag{1.5}$$

The liquid hold up is defined as:

$$R_L = 1 - \alpha = \frac{A_L}{A} \tag{1.6}$$

Mixture density is defined as follows:

$$\rho_m = \alpha\rho_G + (1-\alpha)\rho_L \tag{1.7}$$

The two phase viscosity (μ_{TP}) is:

$$\mu_{TP} = \mu_L(1-\alpha) + \mu_G\alpha \tag{1.8}$$

Superficial gas and liquid velocity is defined as following:

$$V_{SG} = \frac{x\dot{m}}{A\rho_L} \tag{1.9}$$

$$V_{SL} = \frac{(1-x)\dot{m}}{A_L} \tag{1.10}$$

Slip ratio is the relative velocity of the gas phase with respect to the liquid phase.

$$K = \frac{V_G}{V_L} \tag{1.11}$$

Superficial gas and liquid Reynolds number are defined in terms of gas and liquid density, viscosity and superficial gas and liquid velocity as follows:

$$\mathrm{Re}_{SG} = \frac{\rho_G \mathrm{D_i} V_{SG}}{\mu_G} \tag{1.12}$$

$$\mathrm{Re}_{SL} = \frac{\rho_L \mathrm{D_i} V_{SL}}{\mu_L} \tag{1.13}$$

Some of the relevant dimensionless numbers for heat transfer analysis are Nusselt number, which is used to non-dimensionalise the heat transfer coefficient and Prandtl number. Nusselt number is the ratio of convective to conductive heat transfer given as:

$$Nu = \frac{h\mathrm{D_i}}{k} \tag{1.14}$$

Prandtl number is the ratio of the momentum diffusivity to thermal diffusivity given as:

$$\mathrm{Pr} = \frac{\mu c}{k} \tag{1.15}$$

1.2 Flow Patterns

A flow pattern is used to define the flow structure of two-phase flows. Five major type of flow patterns are observed in the upward two-phase flows as shown in Figure 1.1. A brief introduction to these flow patterns is presented here, however a detailed discussion of the flow patterns and their variations with respect to pipe inclination and phase flow rates is given in Section 4.1. Understanding this visual distribution of liquid and gas phase in a two-phase flow is very important to understand the variations in two-phase heat transfer coefficient. The description of these flow patterns are given below:

Bubbly Flow: This flow is characterized by small tiny bubbles dispersed in the liquid phase. For horizontal flow the bubbles tend to be in the upper portion of the pipe due to buoyancy as shown in Figure 1.1(a). Whereas for vertical upward flows the bubbles are more uniformly distributed due to gravity as seen in Figure 1.1(b).

Slug Flow: These slug flows are characterized by large elongated bubbles of gas separated by the liquid slugs. For these flow patterns also the flow structure changes for horizontal pipe orientations and vertical pipe orientations as seen in Figure 1.1 due to the influence of buoyancy and gravitational forces.

Intermittent Flow: These flows consist of slug-wavy and wavy-annular flow regimes. These flows are characterized by the wavy nature of the interface between the liquid and gas layer as shown in Figure 1.1. These flow patterns are observed at moderate gas and liquid flow rates.

Stratified Flow: This flow regime is characterized by the separated flow of gas phase parallel and over the liquid phase has shown in Figure 1.1(a). The gas phase tends to flow on the top of the liquid phase because of the density difference and buoyancy force.

Annular Flow: The flow is usually characterized by the liquid phase forming a continuous thick film on pipe wall encompassing the gas phase as shown in Figure 1.1. The thickness of this liquid layer is subjected to change with respect to changes in pipe orientation as observed in Figure 1.1 (a) and (b) for horizontal pipe flows and vertical pipe flows, respectively

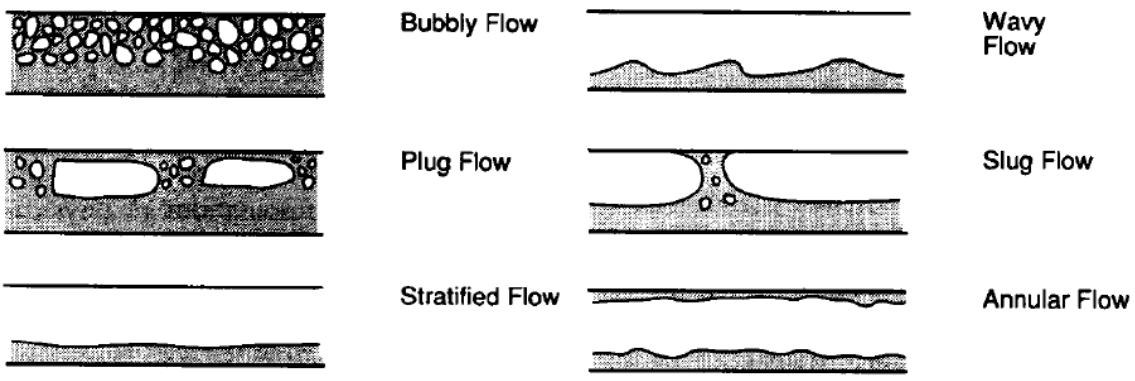

(a)

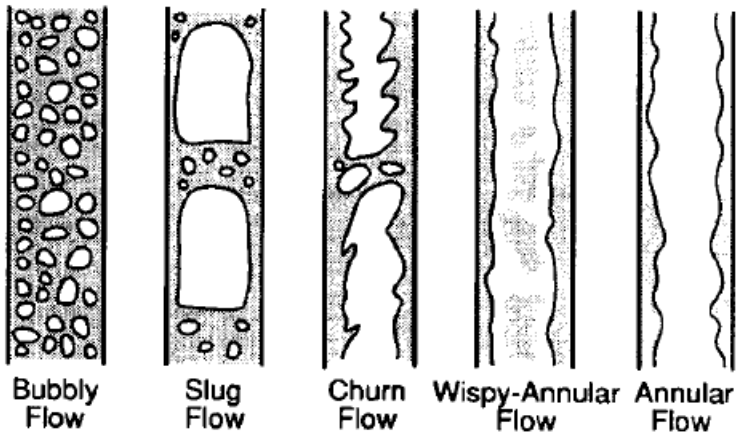

(b)

Figure 1.1 Schematic of flow patterns observed in horizontal gas-liquid flow (Carey (1992))

1.3 Research Objectives

The main objective of this research is to understand the effect of phase flow rates, pipe orientation, pipe diameter and fluid combinations on the two-phase upward flows. In order to achieve this objective measurements of heat transfer coefficients are carried out systematically in-addition to the supplementary flow visualization data. Data from the literature available for different pipe diameters and fluid combinations was also procured. Once the necessary experimental data is collected the effects of changing phase flow rates, pipe orientations, pipe diameters and fluid combinations on the flow patterns and two-phase heat transfer coefficient are analysed. After this a detailed study is under taken to identify heat transfer the correlation that was able to predict these trends of h_{TP} irrespective of phase flow rates, pipe orientations, pipe diameters and fluid combinations. The following tasks are undertaken to achieve these objectives:

(1) Measure h_{TP} in upward pipe inclination at 0^0, $+5^0$, $+10^0$, $+15^0$, $+20^0$, $+30^0$, $+60^0$, $+75^0$ and $+90^0$ and also review the related experimental works to collect additional data for varying pipe diameter and fluid combinations.

(2) Analyse the experimental results with respect to all the variables involved in the flow to establish available heat transfer trends.

(3) Analyse the existing relevant heat transfer correlations for two-phase two-component flows and recommend the best performing correlation.

1.4 Outline

This study is divided into five main chapters providing details on research background, experimental work and analysis used in this work. Chapter II presents a brief review on previous experimental work and also the relevant widely accepted two-phase heat transfer correlations are identified in this Chapter. Chapter III provides a detailed explanation of the experimental setup

used, measurement procedure and the validation of the experimental setup. Chapter IV presents the experimental results and is divided into three parts to incorporate a detailed discussion on flow patterns and flow pattern maps, two-phase heat transfer trend with respect to varying flow parameters and also analyse the performance of different heat transfer correlations identified in Chapter II. Finally, in Chapter V, the conclusions of this work and recommendations for the future work are discussed.

CHAPTER II

LITERATURE REVIEW

Since mid-20th century significant amount of research have been conducted to study the hydrodynamics and transport processes of two-phase gas-liquid flows, which involve both boiling and non-boiling flows but this chapter is however mostly limited to the two-component non-boiling upward flows. The chapter is divided into two parts called "Experimentation in two-phase flows" and "General heat transfer correlations". Since, a comprehensive survey of both experimental and theoretical work done on the subject has been presented by Tang (2011) including extensive bibliography, only the major contributions that have a direct impact on the present investigation will be discussed. The first part of this chapter covers the widely cited experimental works and their results chronologically mainly because some of the data of these authors has been used in the present study. While the second part gives a comprehensive analysis of most widely accepted correlations used for the prediction of two-phase heat transfer coefficient as proposed by the original authors including their limitations.

2.1 Experimentation in Two-phase Flows

One of the earliest two phase flow measurements dates back to Johson and Abou-Sabe (1952), who conducted experiments on air-water flows in a horizontal brass tube of 2.54 cm I.D. and a length of 4.57 m at uniform wall temperature to measure the pressure drop and heat transfer over flow rates ranging from 7.56 to 113 kg/min and 0 to 1.51 kg/min for water and air, respectively.

They observed a significant increase in the heat transfer coefficient when compared to single phase even at the low air flow rate employed in their study.

Groothuis and Hendal (1959) studied the water-air and gas-oil/air mixtures in 1.40 cm I.D. tube with 40 cm long vertical test section and concluded based on their results that the reduction in resistance to the heat transfer was mainly due to the reduction of the thickness of viscous sub-layer at the wall by the wake of the rising air bubbles.

Vijay (1978) undertook an extensive study of two-phase two-component (liquid-air) flows using liquids like water, glycerin (75%)+water (25%) mixture and glycerin to study the changes in heat transfer with respect to the variation in the liquid viscosity and Pandtl number. Their experimental set-up consisted of a heated test section of 11.68 cm I.D. vertical stainless steel tubing type 304 with 61 cm length. This steel tube test section was used as an electrical resistor to generate A.C. Joulean heating because of simplicity involved in measuring and controlling the local heat flux. This heat flux was supplied from a 240 V, 100A, A.C. main power source. The inner wall temperature was measured by determining the outer wall temperature using thermocouples and calculating the temperature drop across the tube wall. The local heat transfer coefficients were integrated axially to measure the mean heat transfer coefficient ($\bar{h}$). The superficial liquid and gas Reynolds numbers spanned over a range of 250 to 126000 and 30 to 163000 for water-air mixture, 8 to 4500 and 43.0 to 100000 for glycerin(75%)+water(25%)-air mixture and 1.8 to 21.0 and 63.0 to 74000 for glycerin-air mixture, respectively. The author concluded that the liquid and air flow rates in-addition to the liquid viscosity effects the flow patterns, which intern strongly effect the mean heat transfer coefficient. It was also observed that the gas phase is flustering the boundary layer, transfers the flow into turbulence increasing the heat transfer coefficient. The author also concluded that high viscosity of the liquid hinder the flow turbulence and there by adversely affecting the mean heat transfer coefficient. But on the

other hand, at high liquid and gas flow rates the mixture velocity increases due to reduction in the area of cross-section available for the flow there by increasing the mean heat transfer coefficient.

Using the same rig as Vijay (1978), Aggour (1978) studied the effect of gas density on the two-phase, two-component flow. The author experimented with water in combination with three different gases like air, helium and feron-12 in vertical tube to allow the change in gas-phase density by a factor of 31. Based on his results a higher mean heat transfer coefficient was noted for the same liquid and gas flow rates with an increase in the gas density. This phenomenon was clearly visualized at moderate to high superficial gas velocities (V_{SG}>1.52 m/s) and low superficial liquid flow rates (V_{SL}<1.04 m/s). These studies were conducted in range of superficial liquid velocity and superficial gas Reynolds numbers varying from 0.3 m/s to 4.5 m/s and 13.95 to 209,000, respectively. Rezkallah and Sims (1987) extended the study of Aggour (1978) and Vijay (1978) in the same vertical tube apparatus to see the effect of reducing the surface tension on heat transfer coefficient using air in combination with three different liquids like water, glycerin(58%)+water(42%) and silicone liquid (5cs viscosity grade). The author concluded that for a given liquid flow rate the mean heat transfer coefficient generally increases with increasing the gas flow rates and this increase is high at low gas flow rates and low at high gas flow rates, which was similar to the conclusion of Vijay (1978) but the only peculiarity was that this trend was common to all the fluid combinations employed in the investigation. The range of superficial liquid and gas Reynolds numbers of different mixtures involved in the study were 4.2 to 1, 27,000 and 52 to 1, 35,000.

Sujumnog (1998) conducted measurements of two-phase mean and local heat transfer coefficients, pressure drop and void fraction for air-glycerin(82%)+water(18%), air-glycerin(59%)+water(41%) and Air-Water flow by varying the liquid Prandtl number from 6 to 766, in-addition to superficial liquid and gas velocities in range of 0.05 to 8.5 m/s and 0.02 to

119 m/s, respectively, to cover almost all the flow patterns in a vertical pipe. The author experimented in the same set-up as the one used by Vijay (1978) and concluded that in general the two-phase mean heat transfer coefficient increases with superficial liquid velocity at any given gas flow rate for all the three air-liquid systems. For Air-Water flows at low liquid flow rates they observed a drop at first followed by an increase in the heat transfer coefficient with increase in the gas flow rate due to formation of the slug flow. The author also reported that for air-glycerin (82%) +water (18%) and air-glycerin (59%) +water (41%) at high liquid flow rates the effect of gas on the mean heat transfer coefficient enhancement is almost negligible but at lower liquid flow rates the increase of the mean heat transfer coefficient with gas flow rate is more pronounced but less than water. The reason for which is attributed to the higher viscosity of the glycerin mixtures compared to the water-air mixture.

Franca et al. (2008) experimented on the convection heat transfer in horizontal gas liquid slug flow in 15 m long, 25 mm I.D. copper pipe for air-water flows and also in 200 m long, 150 mm I.D. steel pipe for natural gas, oil and water flow combinations. They operated with gas and liquid superficial velocities in range of 0.38 to 1.3 m/s and 0.45 to 1.5 m/s, respectively to develop a mechanistic model to predict the slug flow in the two-phase mixture in the actual size pipeline (200 m long, 150 mm I.D. steel pipe) compared to the small scale air-water loop (15 m long, 25 mm I.D. copper pipe).

Tang and Ghajar (2007) conducted a detailed and systematic investigation on the variation of heat transfer coefficient in two-phase non-boiling air-water flows for horizontal and near horizontal inclined pipes. They experimented in 27.9 mm I.D. stainless steel schedule 10S 316 pipe with 2.64 m length of heat transfer section. The test-section was provided with a uniform heat flux from a Lincoln SA-750 arc welder and Miller-Maxtron 450 DC inverter by running high and low amperage DC current through the stainless steel test section respectively. They covered all most

all the flow patterns by measuring 763 data points to include horizontal and near horizontal inclinations of 0^0, $+2^0$, $+5^0$ and $+7^0$. So as to identify the flow pattern shift with respect to inclination and its influence on the two-phase heat transfer coefficient in range of 740 to 26,000 and 560 to 48,000 of superficial liquid and gas Reynolds numbers, respectively. The results suggested that the two-phase heat transfer coefficient was strongly guided by the change in the physical structure of the flow pattern. The authors also observed a considerable increase in the heat transfer coefficient with respect to increase in the inclination from 0^0 to $+5^0$ but as the inclination was even more increased from $+5^0$ to $+7^0$ these effects were reduced. This increase was attributed to the impact of buoyancy, inertia and gravity on the shape of the respective flow pattern as the orientation of the pipe was changed. Similar conclusions were reported by Kalapatapu et al. (2014). They conducted experiments for horizontal and upward inclined flows in range of $0^0 \leq \theta \leq +20^0$. The authors experimented in a 12.5 mm I.D. schedule 10S steel pipe with a length of 80 diameters using Air-Water mixture as working fluid by providing the test section with a uniform wall heat flux from the Lincoln DC-600 welder, which has a maximum current supply of 750 amps to produce 368 data points. Kalapatapu et al. (2014) reported an increase in the two-phase heat transfer coefficient with increase in the superficial liquid Reynolds number and superficial gas Reynolds numbers. They noted that at a given liquid flow rate the heat transfer coefficient increases with a decreasing slope with respect to the increase in the gas flow rate and this effect was found to be influenced by the flow pattern shift and changes in the physical structure of the flow pattern. The authors also concluded that the flow structure is exceedingly dependent on the pipe orientation, which indeed is effecting the shift of the two-phase heat transfer coefficient.

2.2 General Heat Transfer Correlations

Due to the additional complexities in a two phase flow, which has interfacial interactions compared to single phase flows where only wall interactions are seen, it is highly overwhelming to develop a theoretical model from the equations that govern the physics of the fluid because of various factors like liquid holdup and flow reversal. So, several investigators have tended to develop empirical correlations based on the experimental results. Some of the widely accepted correlations in the field of two-phase flow are presented in Table 2.1 and will be reviewed in detail in Section 4.3. One of the earliest but most widely used general two-phase heat transfer correlation comes from Knott et al. (1959), who conducted experiments in a 0.506in I.D. 304 stainless steel vertical tube on oil-nitrogen mixture flowing upward. The setup used a resistance heater to provide constant heat flux boundary condition. Based on the 93 data points they collected over a range of 6.7 to 162 and 126 to 3920 for Re_{SL} and Re_{SG}, respectively, they proposed a two-phase heat transfer correlation (h_{TP}) as shown in Table 2.1. The authors attributed the increase in h_{TP} to the increase in mean velocity of the mixture. Although their correlation is over predicting the experimental values, the authors stated that it is able to predict the approximate trends. However the authors did not report the accuracy of their correlation.

Derresteijn (1970) used the results of Groothuis and Hendal (1959) and performed experiments with oil-air fluid mixture in a vertical tube of 70.00mm I.D. and 110.00cm long. Their aim was to study the effect of tube size on the heat transfer coefficient. The study was conducted for the superficial liquid Reynolds number range of 300 to 66,000. Based on these results the author was able to conclude that for a larger tube size, the heat transfer coefficient was much lower compared to the data in the smaller pipe of 70.00mm I.D. This study also involved both upward and downward flows from which they suggested that the flow direction has no effect on the two-phase heat transfer coefficient. Based on these results the author has proposed a correlation as

shown in Table 2.1, while the exact percentage of points predicted by the correlation in a specified error bands was not reported.

Martin and Sims (1971) studied air-water flows in horizontal rectangular channel with 0.52in x 0.257in cross-section and 0.52in height by injecting the air through porous heated wall. Based on the 52 data points that encompasses all flow patterns from slug to annular, they developed a general heat transfer correlation as given in Table 2.1 to predict 88% of their measured data within ±20%. Similar experiments was performed by Khoze et al. (1976) over a wide range of fluid viscosity by using air-water, air-Diphenlyoxide and air-Polymethylsiloxane flowing through a rectangular channel to develop their heat transfer correlation given in Table 2.1. This correlation predicted 100% of the data within ±20%. The data was collected in a range of 4000 to 37,000 and 3.5 to 210 for superficial gas and liquid Reynolds numbers, respectively.

Aggour (1978) using 338 experimental data points of water-air, water-helium and water-feron12 measured as mentioned earlier in section 2.1, proposed two correlations one for laminar and one for turbulent flows. These correlations are based on the same form as that of single phase heat transfer correlations and are given in Table 2.1. The author while developing the correlation assumed that the introduction of gas phase act to accelerate the liquid phase in the test section and heat transfer is mainly by the liquid phase. This correlation predicted 91% of 338 data points within ±50%.

Ravipudi and Godbold (1978) used air-water, air-toluene, air-benzene and air-methanol as gas-liquid combinations in vertical steam condenser and collected data in superficial gas and liquid Reynolds number ranges of 3500 to 820000 and 85000 to 90000, respectively. The authors aimed to investigate the effect of mass transfer rates on heat transfer coefficient and concluded that as the mass transfer rate from liquid to gas increases the heat transfer rate increases, whereas the heat transfer coefficient decreases. They also compared the data of different fluid combinations at the same Re_{SL} and found out that the effect of surface tension on two-phase heat transfer is

negligible. Based on these results they developed a correlation as given in Table 2.1. However, the exact percentage of data points that fell within ±20% and ±30% error bands was not reported in the literature.

Chu and Jones (1980) conducted experiments on vertical upward and downward air-water flows in a tube of 2.67cm I.D. and a length of 34 times the inner diameter under constant heat flux. They attempted to examine the impact of flow direction on heat transfer and found that downward flow has higher heat transfer coefficient compared to upward flow for the same superficial velocities of air and water. The authors attributed the reason for increased heat transfer in downward flow to the higher liquid velocities because of higher void fractions than those observed in the upward flow. These observations are recorded in 16000 to 112000 and 540 to 2700 ranges of superficial liquid and gas Reynolds numbers, respectively. They developed a correlation based on this data by incorporating the ratio of atmospheric pressure to system pressure for the purpose of accounting for the pressure changes in the system as seen in Table 2.1. This correlation was able to predict 100% of data within ±15%.

Shah (1981) worked on 672 data points collected from horizontal and vertical channels with circular and non-circular cross-sections. This data is acquired from 10 liquid-gas mixture combinations involving a combination of air with water, oil, nitrogen and glycol. The data was from both horizontal and vertical channels with circular and non-circular tubes involving a hydrodynamic diameter ranging from 4mm to 70mm with a wide range of heat and mass flux. The author correlated the data in a similar way to single-phase heat transfer theory and developed a heat transfer correlation as given in Table 2.1. This correlation was able to predict 96% of the data within ±30% error band.

Drucker et al. (1984) conducted experiments on vertical flow inside the tube and also for the flow over rod bundles with blockages using air-water as working fluid. Based on existing heat-transfer data for the air-water flows inside the vertical tube with liquid Reynolds number ranging from

2,000 to 1,50,000 and void fraction up to 0.4, the authors proposed a heat transfer correlation which is a function of Gr/Re^2 and void fraction as given in Table 2.1. This correlation was able to predict most of the data collected by the authors with in ±35%.

Oshinowo et al. (1984) experimented on air-water flow in a 25.8mm I.D. vertical pipe at 172Kpa pressure by varying the liquid volumetric ratio and superficial liquid Reynolds number from 2 to 220 and 1700 to 5600, respectively. This experiment involved both upward and downward flows from which the authors observed that the upward flows generally have higher heat transfer coefficients than the downward flows at similar liquid and gas flow rates. Based on this data the authors proposed a correlation for the heat transfer coefficient of both upward and downward flows as given in Table 2.1. This correlation was able to predict mostly all of their data with ±18%.

Rezkallah and Sims (1987) tested eleven of the existing correlations using 64 water-air data points, 124 glycerin+water-air data points and 190 silicone-air experimental data points as mentioned earlier in section 2.1. The authors reported that many of the correlations performed reasonably well for most of the data but for high Prandtl number fluids like glycerin where existing correlations failed to perform reasonably well, the authors proposed a correlation for the mean heat transfer coefficient by compensating the single-phase heat transfer of Siedar and Tate (1936) using void fraction as given in Table 2.1. This correlation was able to predict all data of the glycerine+water-air within an error band of ±50%.

Kim and Ghajar (2006) studied non-boiling air-water flows at uniform heat flux in a horizontal pipe to observe the effect of flow pattern on heat transfer. By experimenting in a stainless steel tube of 27.9mm I.D. with a length to diameter ratio of 100 they collected 114 data points to include almost all the flow patterns. The authors have concluded that the two-phase convective heat transfer is strongly influenced by the liquid phase because at a constant liquid superficial velocity there is a weaker dependency on the gas superficial velocity. They have also shown that

each flow pattern plug, slug, slug/wavy, annular and bubbly have their own distinguished heat transfer trends by analyzing the above data points collected at superficial gas and liquid Reynolds numbers ranging from 560 to 48000 and 820 to 26000, respectively. Based on this data they developed a correlation to predict the two-phase heat transfer coefficient as shown in Table 2.1 by assuming that the gas-liquid two-phase heat transfer is the sum of the individual single phase heat transfer of gas and liquid weighted by volume of each phase. This correlation involves a flow pattern factor that takes the effective wetted perimeter into account to overcome the flow pattern effect on heat transfer. They carefully derived this heat transfer correlation using the cross-sectional areas occupied by both liquid and gas phases, to take into consideration the respective contribution of each phase to the heat transfer. This correlation was able to predict 93% of the authors' data within ±20% deviation.

Tang and Ghajar (2007) proposed a very practical correlation by modifying the work of Kim and Ghajar (2006), which in-fact is a modification of Sieder and Tate (1936) for single phase flow. They undertook an extensive study by collecting 763 air-water data points measured at 0^0, $+2^0$, $+5^0$ and $+7^0$ as mentioned earlier in section 2.1 and found out that inclination has a profound effect on the interaction of different forces in the pipe, which effects the flow pattern and heat transfer. They also noticed that the density difference between gas and liquid causes the denser liquid phase to be affected more by the inclination of the pipe. Based on these observations to account for the relative force acting on the liquid phase in the flow direction due to inertia and the gravitational force the authors introduced the inclination factor (I) and proposed a correlation as given in Table 2.1. This correlation was capable of predicting heat transfer coefficients in two-phase flow regardless of the pipe orientation, pipe diameter, fluid combination and flow pattern. The proposed correlation makes use of both inclination factor(I) and flow pattern factor(F_P) introduced by Ghajar and Kim (2005) and is able to predict 85.6% and 75% of the 763 measured data points within the range of ±30% and ±20%, when Spedding and Chen (1984) void fraction

correlation was used. Although the authors ignored the influence of the surface tension and the contact angle of each phase on the effective wetted perimeter, at the current state of knowledge this correlation may be considered the most robust in handling interactions between the phases for varying inclinations.

The selected correlations which are going to be used for the performance evaluation of the current research are tabulated in Table 2.1.

Table 2.1 List of selected correlations for the heat transfer data analysis

Authors	Correlations	Range, Fluids used and Applicability	
Knott *et al.* (1959)	$\frac{h_{TP}}{h_L} = (1 + \frac{V_{SG}}{V_{SL}})^{\frac{1}{3}}$ $h_L = 1.86(\frac{k}{D_i})(Re_{SL}Pr_L \frac{D_i}{l})^{\frac{1}{3}}(\frac{\mu_b}{\mu_w})^{0.14}$	Range	$6.7 \leq Re_{SL} \leq 162$ $126 \leq Re_{SG} \leq 3920$
		Fluids	Oil-nitrogen mixture
		Applicability	Vertical tubes with 0.506in I.D.
Dorresteijn (1970)	$\frac{h_{TP}}{h_L} = (1 - \alpha)^{-n}$ where n given as = 0.33 for laminar flow and 0.8 for turbulent flow and single phase heat transfer coefficient is given by $h_L = 0.0123\ {Re_{SL}}^{0.9} {Pr_L}^{0.33} \left(\frac{\mu_b}{\mu_w}\right)^{0.14} (\frac{k}{D_i})$	Range	$0.02 \leq V_{SL} \leq 4.6$
		Fluids	Oil-air mixture
		Applicability	Vertical tube with 70mm I.D.
Martin and Sims (1971)	$\frac{h_{TP}}{h_L} = 1 + 0.64(\frac{V_{SG}}{V_{SL}})^{\frac{1}{2}}$ where h_L is from Sieder and Tate (1936) is given in Table 3.3.	Fluids	Air-water mixture
		Applicability	Horizontal rectangular channel with hydraulic diameter of 0.343in.
Khoze *et al.* (1976)	$Nu_{TP} = 0.26\ {Re_{SG}}^{0.2} {Re_{SL}}^{0.55} {Pr_L}^{0.4}$	Fluids	Air in combination with water, diphenyloxide and polymethylsiloxane .
		Range	$3.5 \leq Re_{SL} \leq 210$ $4000 \leq Re_{SG} \leq 37000$
Aggour (1978)	$\frac{h_{TP}}{h_L} = (1 - \alpha)^{-\frac{1}{3}}$ (Laminar) $h_L = 1.615(\frac{k}{D_i})\ (Re_{SL}Pr_L \frac{D_i}{l})^{\frac{1}{3}}(\frac{\mu_b}{\mu_w})^{0.14}$	Range	$0.3 \leq V_{SL} \leq 4.5$ $13.9 \leq Re_{SG} \leq 209000$

Authors	Correlations	Range, Fluids used and Applicability	
	$\frac{h_{TP}}{h_L} = (1-\alpha)^{-0.83}$ (Turbulent) $h_L = 0.0155(\frac{k}{D_i})Re_{SL}^{0.83}Pr_L^{0.5}(\frac{\mu_b}{\mu_w})^{0.33}$	Fluids	Combination of water with air, helium and Feron12
		Applicability	Vertical tube with 11.8mm I.D.
Ravipudi and Godbold (1978)	$Nu_{TP} = 0.56{Re_{SL}}^{0.6}{Pr_L}^{0.33}(\frac{\mu_b}{\mu_w})^{0.14}(\frac{\mu_G}{\mu_L})^{0.2}(\frac{V_{SG}}{V_{SL}})^{0.3}$	Range	$8500 \leq Re_{SL} \leq 90000$ $3500 \leq Re_{SG} \leq 820000$
		Fluids	Combination of air with toluene, benzene and methanol
		Applicability	Vertical steam condenser
Chu and Jones (1980)	$Nu_{TP} = 0.43{Re_{SL}}^{0.55}{Pr_L}^{0.33}(\frac{\mu_b}{\mu_w})^{0.14}(\frac{Pa}{P})^{0.17}$	Range	$16000 \leq Re_{SL} \leq 112000$ $540 \leq Re_{SG} \leq 2700$
		Fluids	Air-water mixture
		Applicability	Vertical flows with 2.67cm I.D.
Shah (1981)	$\frac{h_{TP}}{h_L} = (1+\frac{V_{SG}}{V_{SL}})^{\frac{1}{4}}$ $h_L = 1.86(\frac{k}{D_i})(Re_{SL}Pr_L\ \frac{D_i}{l})^{\frac{1}{3}}(\frac{\mu_b}{\mu_w})^{0.14}$ (Laminar) $h_L = 0.023(\frac{k}{D_i}){Re_{SL}}^{0.8}{Pr_L}^{0.4}(\frac{\mu_b}{\mu_w})^{0.14}$ (Turbulent)	Fluids	Combination of air with water, oil, nitrogen and glycol
		Applicability	Vertical and horizontal circular and non-circular tubes with hydraulic diameter ranging from 4 to 70mm.
Drucker *et al.* (1984)	$\frac{h_{TP}}{h_L} = 1 + 2.5\,(\frac{\alpha Gr}{{Re_{TP}}^2})^{0.5}$ $Gr = \frac{(\rho_L - \rho_G)gD_i^{\,3}}{\rho_L {v_L}^2}$	Range	$2000 \leq Re_{SL} \leq 150000$ Void fraction up-to 0.4
		Fluids	Air-water mixture
		Applicability	Vertical tubes

Authors	Correlations	Range, Fluids used and Applicability	
Oshinowo et al. (1984)	$Nu_{TP} = 1.2Re_{SL}^{0.6}Pr_L^{0.33}(\frac{\mu_b}{\mu_w})^{0.14}(\frac{\mu_G}{\mu_L})^{0.2}(\frac{V_{SG}}{V_{SL}})^{0.1}$	Range	$54 \leq G_L \leq 172$ $540 \leq j_G \leq 1.322 \times 10^{-2}$
		Fluids	Air-water mixture
		Applicability	Vertical pipes in 25.8mm I.D.
Rezkallah and Sims (1987)	$\frac{h_{TP}}{h_L} = (1-\alpha)^{-0.9}$ where h_L is from Sieder and Tate (1936) given in Table 3.3.	Fluids	Air-glycerin mixture
		Applicability	Vertical tube with 11.8mm I.D.
Kim and Ghajar (2006)	$\frac{h_{TP}}{h_L} = F_P\{1 + 0.7(Z)\}$ Where $Z = \left(\frac{x}{1-x}\right)^{0.08}\left(\frac{1-F_P}{F_P}\right)^{0.06}\left(\frac{Pr_G}{Pr_L}\right)^{0.03}(\frac{\mu_G}{\mu_L})^{-0.14}$ $F_P = (1-\alpha) + \alpha[\frac{2}{\pi}(tan^{-1}\sqrt{(\frac{\rho_G\,(V_G-V_L)^2}{gD_i(\rho_L-\rho_G)})}]^2$ h_L is determined by Sieder and Tate (1936) equation given in Table 3.3.	Range	$820 \leq Re_{SL} \leq 26000$ $560 \leq Re_{SG} \leq 48000$
		Fluids	Air-water mixture
		Applicability	Horizontal pipes with 27.9mm I.D.
Tang and Ghajar (2007)	$\frac{h_{TP}}{h_L} = F_P\{1 + 0.55(P)\}$ *Where* $P = \left(\frac{x}{1-x}\right)^{0.1}\left(\frac{1-F_P}{F_P}\right)^{0.4}\left(\frac{Pr_G}{Pr_L}\right)^{0.25}(\frac{\mu_L}{\mu_W})^{0.25}I^{0.25}$ $F_P = (1-\alpha) + \alpha[\frac{2}{\pi}(tan^{-1}\sqrt{(\frac{\rho_G\,(V_G-V_L)^2}{gD_i(\rho_L-\rho_G)})}]^2$ $I = 1 + \frac{[(\rho_L-\rho_G)gD_i{}^2\lvert sin\,\theta\rvert]}{\sigma}$ where h_L is from Sieder and Tate (1936)	Range	$740 \leq Re_{SL} \leq 26000$ $560 \leq Re_{SG} \leq 48000$
		Fluids	Air-water mixture
		Applicability	0^0, 2^0, 5^0 and 7^0 inclined tubes with 27.9mm I.D.

From above review of the existing literature in the two-phase flow, it is clear that majority of the work pertaining to two-phase heat transfer is concentrated to either horizontal or vertical orientations of the pipe and even is limited to certain flow patterns in many cases. Also, it can be observed that many of the prominent correlations didn't account for the pipe orientation, flow pattern change, pipe diameter and fluid combination. It can also be noticed that not all the correlations included the effects of interactions between the phases completely, which are shaped by viscosity, buoyancy, gravity, inertial and surface tension forces. Having listed the general heat transfer correlations in Table 2.1, some of the best performing correlations are analyzed with present data and also with certain data sets from the literature, which include Vijay (1978), Aggour (1978), Rezkallah and Sims (1987), Sujumnong (1998), Franca et al. (2008), Tang and Ghajar (2007) and Kalapatapu et al. (2014) in Chapter IV.

CHAPTER III

EXPERIMENTAL SETUP

The present experimental set-up is at Oklahoma State University Two-phase Flow Laboratory and was designed by Cook (2008) to permit flow visualization in-addition to the measurements of void fraction, pressure drop and heat transfer. The set-up consist of two separate test branches for the above mentioned purposes. One of them allows for flow visualization and void fraction measurements as shown in the left of Figure 3.1 (front view), whereas the other one shown on the right in the Figure 3.1 (front view) allows for pressure drop and the heat transfer measurements. The scope of the below discussion will be limited only to heated test section and its components because the subject of present study is two-phase heat transfer in upward orientation. However, a detailed discussion of the experimental setup can be found in Cook (2008). This chapter is mainly divided into four parts, firstly in Section 3.1 we deal with the details of experimental setup to cover all the parts in the experimental circuit and in Section 3.2 we deal with various instruments used in the measurement and collection of data. In Sections 3.3 and 3.4 we deal with experimental procedure and validation of experimental setup respectively.

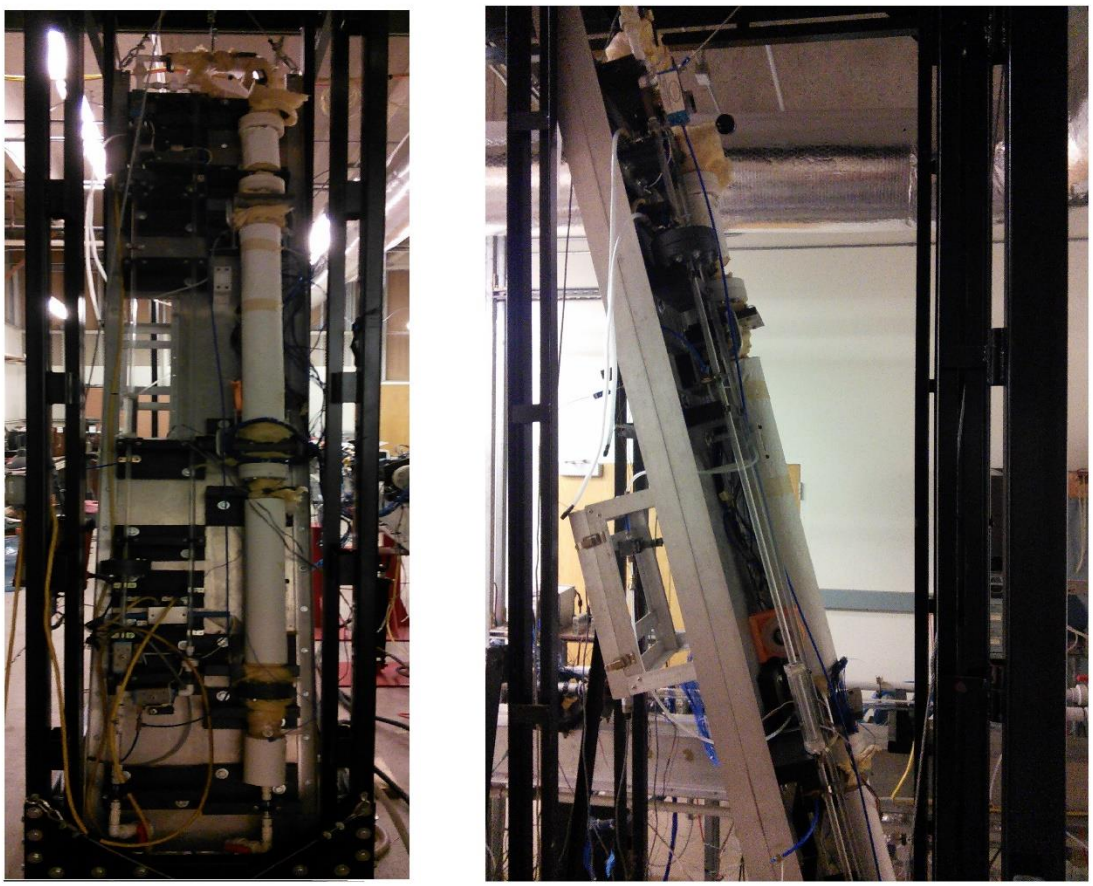

Front View Side View

Figure 3.1 Photograph of experimental setup at $+75^0$

3.1 Details of Experimental Setup

Flow Loop: The overall systematic representation of experimental setup is given Figure 3.2. Both flow visualisation and the stainless steel pipe test sections rest on an aluminium I-beam platform measuring 3.353m in length and 0.61m in width. The test sections are fastened to the platform using a combination of 5.08cm x 15.24cm blocks and leather strapping, which indeed is attached to variable inclination frame to allow inclinations varying in a range of $+90^0$ to -90^0. This variable inclination frame consists of a heavy outer frame and a lighter

internal rolling frame. The heavy outer frame is made of regular steel tubing to have a 4.57m length, 3.66m height and 0.84m in width. This outer frame is equipped with an extra length to allow for any further additions and is bolted to the floor to provide rigidity and stability of the test-section. The inner rolling frame is also made out of steel tubing and is fastened to the rolling frame with a bolt and plastic bushing combination. A slot of 3.175m and 38.1mm is cut lengthwise in the variable test section and is used to allow for positive and negative inclinations. The inclination angles were measured with a contractor's angle measuring tool.

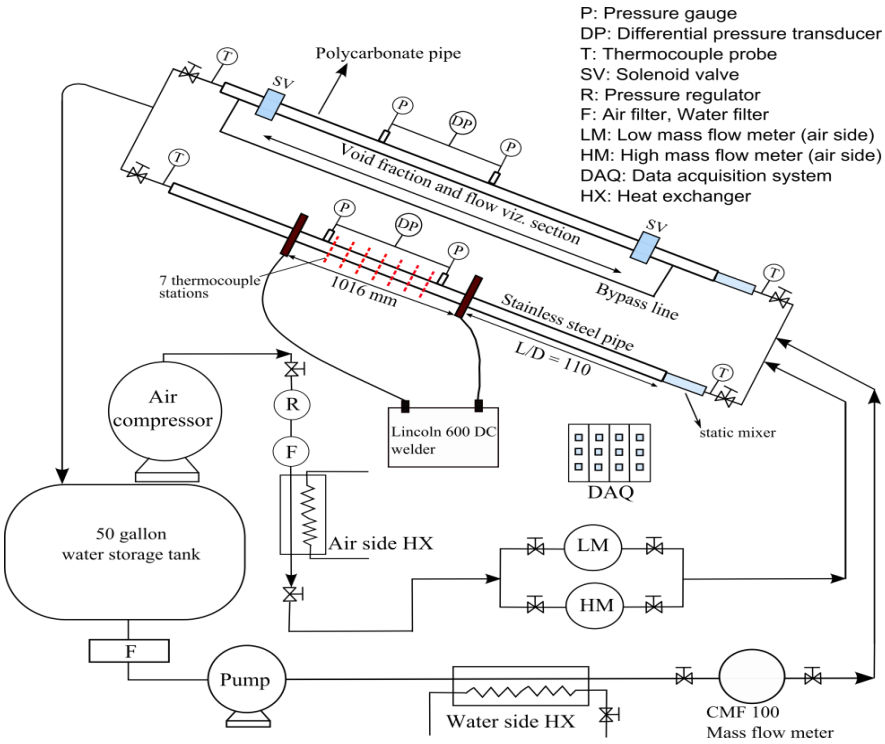

Figure 3.2 Schematic of experimental setup

Supply of Working Fluids: Air and distilled water are the working fluid used for the present study, even though the system is capable of handling other liquids like glycerine. The water used in this research is purified from organic chemicals, chlorine and is passed through an ultraviolet lamp for sterilizing any microbes using the reverse osmosis technique. This water is then stored in a 55 gallon polyethylene tank that acts as a reservoir from where the water is supplied using a

Bell and Gosset (series 1535) centrifugal pump. The pump sucks the water through an Aqua-pure AP 12T water purification system to trap foreign objects and organic impurities. The temperature of the distilled water is controlled using an ITT standard (Model BCF 4063) one shell and two tube heat exchanger, which employs tap water taken directly from the wall tap as a coolant. This water then flows through the micro motion (model CMF125) Coriolis flow meter, where the water flow is controlled by using a gate valve located just after the flow meter assembly. This water is then mixed with the air supply as it passes through one of the test sections before being finally returned to the polyethylene reservoir. Ingersold-Rand TB0 (Model 2545) air compressor supplies the air, which is regulated by Speedaire (Model 42M22) regulator. The compressor can deliver a maximum flow rate of 0.25kg/min at a maximum pressure of 826KPa. This air is cooled by passing through a copper coil submerged in tap water, which is also used for cooling the distilled water to ensure the same inlet temperature for both fluids. Then the air passes through Speedaire (Model 47149) air filter to remove the moisture. This air is then flowed through Parker Model 24NS 82(A)V8LN-SS needle valve regulator to regulate the air flow before being passed through Emerson Flow Meter (Micro Motion Elite series Model number LMF 3M and CMF025).

Air Water Mixing Section: Air and water are carried to the test section via reinforced flexible tubing. Two different mixing sections Koflo 3-Vane static mixer (Model 3/8-40C-4-3V-2) and Koflo (1/2-80-4C-3-2) are used in the heated section to help mixing, one at the inlet and another at the outlet of the test section respectively. The mixers' job is to ensure the proper mixing of air and water that enter the test area via IPS Plastic tree to assure the accuracy of the temperature read by the thermocouple probes in-addition to nullification of the influence by inlet configuration on the flow.

Heat Source: Lincoln DC-600 three phase rectified electric welder is used to provide uniform wall heat flux to the test section by supplying high amperage DC current through the stainless steel test section. The Lincoln DC-600 welder is capable of producing steady output current up-to

750Amp. A 1000Amp shunt manufactured by Empro shunts (Model number: B-1000-50.2) has been connected on the connection plate in-line with the circuit at the exit of the heated test section. A 4/0 AWG welding cable is used in connecting the plates to the welder.

Heat Transfer Test Section: The test section is made of 3/8in nominal schedule 304 stainless steel pipe of roughness 0.0152mm. The tube has 12.52mm internal diameter (I.D.) with length of 80 diameters or 101.6cm. A 17.8cm x 17.8cm large copper plates of 6.35mm thick were silver soldered at either end of the test section to provide electrical connections and these plates completely encircle the test section in order to achieve an even distribution of current input. A thick phenolic resin board of 1.27cm is used on the sides of the plates that faces away from the heated section in-order to prevent heat loss from the heated test section. The non-isothermal pressure drop is measured by the pressure taps installed at both ends of the test section, which are connected to a Validyne pressure transducer. A 0.076m thick Micro-Lok fibre glass insulation with thermal conductivity of 0.042w/m^{0}C is used as an insulation in order to prevent heat loss from the test section to the surrounding.

3.2 Instrumentation

Flow Rate Measurement: The water flow rate is measured by the Micro Motion (Model CMF 100) Coriolis flow meter as shown in Figure 3.3 (Water Mass Flow Meters) with an accuracy of ±0.05% and the air flow rate is measured by Emerson flow meters (Micro motion Elite series Model number LMF 3M and CMF025) as shown in Figure 3.3 (Air Mass Flow meters) with an accuracy of ±0.20%. The water flow meter and air flow meter has the capacity to measure in ranges of 1360 kg/hr to 27200kg/hr and 54kg/hr to 2180kg/hr, respectively. The water flow meters uses Micro Motion Model RFT9739 field mount transmitter to display the flow rate readings, flow properties and also to transmit this information to data acquisition system, whereas the air flow meters employ Micro Motion Model 1700 transmitter to do the same functions.

Water Mass Flow Meters Air Mass Flow Meters

Figure 3.3 Photograph of Flow meters

Temperature Measurement: Two Omega TMQSS-1250-6 thermocouple probes are stationed at the inlet and outlet of the test section to measure the temperature of the mixture before and after the test section. In-addition, there are seven Omega TT-T-30 T-type thermocouple stations with four thermocouples in each station to measure the outer wall temperatures accurately. These stations are placed 127mm apart along the pipe length to have the four thermocouples each placed symmetrically at 45^0 apart as shown in Figure 3.4 to measure the temperature along the circumference and also along the length of the pipe. These thermocouples are cemented to the test section using Omega bound 101 and can measure temperature in the range of -250^0C to 350^0C with an accuracy of ±1.0 ºC (1.8 ºF) or ±0.75% of the measured value. The thermocouple probes and thermocouples are connected with the data acquisition system through Omega 24 gauge type T thermocouple wire.

Figure 3.4 Circumferential positioning of thermocouples

Pressure Measurements: A Validyne DP15 differential pressure transducer along with Validyne CD15 carrier demodulator is used for measuring pressure drop across the test section between the first and the last pressure taps. Both non-isothermal and isothermal pressure drops can be measured with an accuracy of ±0.25% using the heated section and flow visualization section. This equipment has the capacity to measure pressures ranging from 0.862kPa to 1379kPa. The Validyne CD15 carrier demodulator receives the output signals from the differential pressure transducer that is to be demodulated, amplified and filtered. These signals are then sent from demodulator to data acquisition system for data recording.

Power Measurements: The voltage drop across the heated test section is recorded by the data acquisition system and determined by the copper shunt attached to the setup at the downstream of the test section. The current flowing through the test section can be determined by the measured voltage drop from the copper shunt and the resistance across the shunt. Using this current calculated from voltage drop and the resistance, heat flux is determined. A heat balance analysis is done for the heat flux based on the electrical input and thermal output to assure the accuracy of the system. This heat balance error is given as the percentage difference between the heat input rate from the welder and heat transfer rate calculated by using the enthalpy equation for the flow, calculated as shown below:

$$\text{Heat input rate, } \dot{q} = V_D I \tag{3.1}$$

$$\text{Heat rate from enthalpy, } \dot{q} = \dot{m} c (T_{b,out} - T_{b,in}) \tag{3.2}$$

$$\text{Heat balance error (\%)} = \frac{Heat\ rate\ from\ enthalpy - Heat\ input\ rate}{Heat\ input\ rate} \times 100 \tag{3.3}$$

Data Acquisition System: This is a crucial part of the facility where the data acquired from the setup is recorded in the Central Processing Unit using National Instruments data acquisition system. This data acquisition system has three main units called Chassis, Modules and Terminal block. The Chassis (SCXI 1000) is used to provide a low noise environment for signal

conditioning, power supply and circuitry controls. This is powered by alternating current and houses all the components of the data acquisition system. Four slots for Modules and accompanying terminal blocks were provided in the Chassis. Modules provide signal conditioning and are connected directly with the chassis to which the terminal blocks are attached. Two 32 channel Analogue Modules (SCXI 1102) and one eight channel analogue Module (Model SCXI 1125) are used to procure data from the setup, especially from the thermocouples by using a 2Hz low pass filter. The terminal blocks are attached to these modules through screw terminals and are used to provide direction connection for the thermocouples, pressure transducers and the Coriolis flow meters. The graphical interface program is achieved by Labview from National Instruments. The Labview program for this setup was developed by Clement Tang (former Ph.D. student) based on the original code written by Jae Yong Kim (former Ph.D. student).

3.3 Experimental Procedure

In order to obtain the repeatability of experimental data and proper functioning of the equipment and experimental setup it is important to stick to predefined experimental procedure. In order to discuss the experimental procedure this section is categorised into three different parts named as Stat-up procedure, Measurement procedure and Data reduction.

Start-up Procedure: The aim of this procedure is to catalogue several steps to start the experimental setup and make provisions for conducting measurements safely by checking for proper operations.

1) Firstly, adjust the inclination by using the variable inclination frame and check the heated section test section to make sure that both the inlet and outlet valves are open. After this, electrical instruments like air compressor, data acquisition system, Coriolis flow meters and Validyne CD15 carrier Demodulator should be turned ON.

2) The second step is to check air and water filter for clogs to ensure proper working and turn ON the heat exchanger to allow the stabilization of the temperature of both incoming air and water to the system. The coolant employed in the heat exchanger is tap water and this is sufficient to normalize the temperature of the working fluids to the room temperature. After this the lab-view program is executed and thermocouple readings in the test section are checked in-addition to both outlet and inlet temperatures measurements of the mixture by thermocouple probes. This step also involves checking the test section for any leaks.
3) Check all the electrical connections of the D.C. welder and copper plates to ensure good condition and also make sure the temperature of the mixture and the thermocouples are stable before turning the welder on. Check the insulation and adjust the current to provide constant heat flux to the tube wall. At the same time avoid any dry spots that can cause damage to the system because of overheating of the metal. Also, check for any lose connections in the welder system to avoid fire hazards or over heating that can cause damage to the system.

Measurement Procedure: The below discussion consist of steps to successfully obtain quality and accurate data.

1) Adjust water and air flow to desire value using the Coriolis flow meters. Once the required flow rates is reached run the Labveiw Virtual Instrument (VI) program to monitor the welder current and voltage, air flow rate, water flow rate, system pressure, inlet and outlet temperatures of the Air-water mixture and the thermocouples stations temperatures as shown in Figure 3.5.
2) Check if the inlet and outlet temperatures of the fluid mixture are stable and are almost at a similar values to minimize the heat balance error. Then turn the welder ON and adjust

the current to achieve a temperature difference of almost around 4^0C between the inlet and outlet temperature of the fluid mixture.

3) Monitor the Labveiw Virtual Instrument (VI) program to make sure the inlet and exit thermocouple probes has reached a steady state and also make sure that none of the thermocouple at the temperature station has reached a temperature above 60^0C to avoid local boiling of the flow mixture, which can result in dry spots.
4) After ensuring the above precautionary measures, record the data by using the RECORD DATA button in Labveiw VI program as shown in Figure 3.5. The time for recording the data is strongly dependent on flow pattern. For flows where high uncertainty and heat balance error is common like intermittent, stratified and annular a high recording time in the range of 8-10 minutes is proposed. Similarly, for flow patterns with moderate to low uncertainty and heat balance error like bubbly and slug a moderate recording time in the range of 4-6 minutes is proposed. The recording time ranges are proposed based on general observations and also from past recommendations of Mollamahmutoglu (2012) and Kalapatakapu et al. (2014).
5) After recording the data turn the DC welder OFF and allow the test section to cool down by letting the fluid mixture take the heat. This heat is again transfered from the fluid mixture to the coolant in the heat exchanger. Then repeat the above steps to collect data again.
6) After completion of the data collection to shut down the facility to stop Labveiw VI program and data acquisition system. Turn the D.C. welder, Coriolis flow meter, heat exchanger and air compressor OFF. Set the D.C. welder and Coriolis flow meter to the minimum value possible.

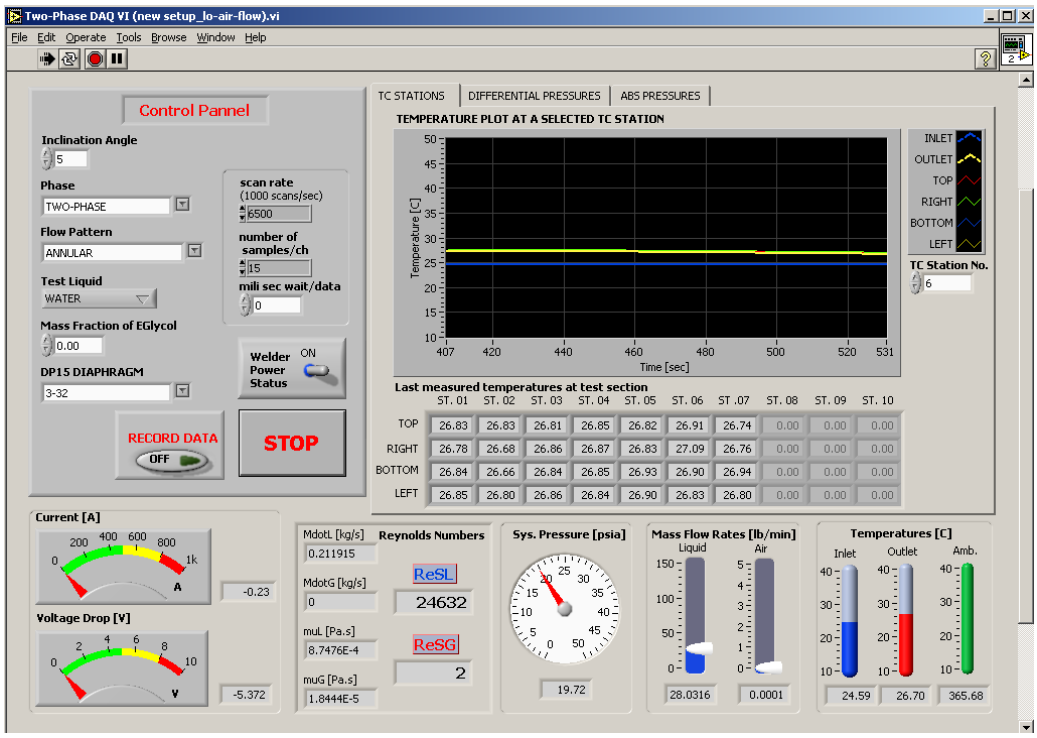

Figure 3.5 Graphical user interface of the LabVIEW Virtual Instrument (VI) program

Data Reduction: The outside pipe wall temperature is calculated using thermocouple stations and also the bulk fluid temperatures at inlet and outlet are measured using thermocouples probes. The heat generation is known from the current and voltage provided by D.C. Welder. Based on this the local inside wall temperature, local bulk fluid temperature, local wall heat flux and both local and overall heat transfer coefficients are calculated by applying a finite difference method on a control volume. This process is achieved by employing the data reduction program originally developed by Ghajar and Kim (2006) and later modified by Clement Tang (a former Ph.D. student) for the present setup. Local average heat transfer is integrated along the pipe to calculate the overall heat transfer coefficient as shown in Equation (3.4) and then the Nusselt number is obtained using Equation (3.5).

$$h = \frac{1}{l}\int \bar{h}\,dz = \frac{1}{l}\sum_{j=1}^{N_{ST}} \bar{h}_j \Delta z_j \qquad (3.4)$$

$$Nu = \frac{hD_i}{k} \tag{3.5}$$

It should be noted that this program is developed by assuming steady state condition with only radial and circumferential conduction by neglecting axial conduction. The data reduction program also assumes that the electrical resistivity and thermal conductivity in the pipe wall are functions of the temperature. The heat balance error is also calculated by the data reduction program and is desired to be less than 10% to ensure reliability and accuracy of the data collected.

3.4 Validation of the Experimental Setup

The validation of the experimental setup was done by checking the uncertainty associated with the measured flow data and also by comparing the measured single phase heat transfer coefficient with respect to widely accepted single phase heat transfer correlations in-addition to the comparison of some of the present experimental data to already existing past works. The first part of this section deals with the uncertainty analysis of the two-phase flow measurement. While the consecutive sections deals with comparison of the single phase heat transfer coefficient with preselected correlations and testing for the repeatability of the data using the past data at comparable flow rates.

Two Phase Heat Transfer Uncertainty: In-order to validate the accuracy and repeatability of the experimental setup an uncertainty analysis was done for the two-phase heat transfer measurements using the method proposed by Kline and McClintock (1953). The details of the uncertainty analysis performed was given in Appendix A. Table 3.1 shows the uncertainty associated in the measurement of two-phase heat transfer coefficient and other associated two-phase flow variables for a worst case scenario. The minimum and maximum uncertainty associated in the measurements of two-phase heat transfer coefficient at each observed flow pattern are presented in Table 3.2.

Table 3.1 Uncertainty in measured values of two phase heat transfer coefficient (worst case scenario)

Variable	Value	± Uncertainty	± % Uncertainty
Inner pipe diameter (m)	0.01252	0.0000127	0.1
Outer pipe diameter (m)	0.0171	0.0000127	0.07
Heat transfer length (m)	0.889	0.003175	0.31
Thermal conductivity (W/m-K)	13.438	-	-
Current (I)	231.83	2.32	1.00
Voltage (V)	1.55	0.02	1.00
Inner wall temperature (^oC)	14.11	0.50	3.55
Heat transfer rate (W)	375.87	5.08	1.35
Heat transfer coefficient (W/m^2 K)	2998.31	907.12	30.25

Table 3.2 Minimum and maximum uncertainty in measured h_{TP} for different flow patterns

Flow pattern	Minimum uncertainty (%)	Maximum uncertainty (%)	Average uncertainty (%)
Stratified	15.08	24.81	20.05
Slug	5.68	13.49	11.08
Intermittent	6.08	28.81	15.33
Bubbly	5.7	12.31	9.55
Annular	6.19	30.25	18.72

It can be seen from Table 3.2 that higher magnitude of uncertainty is a observed in annular, intermittent and stratified flow patterns compared to other flow patterns like bubbly and slug because of the inability to maintain higher temperature difference between the test-section inlet and exist thermocouple probes and also due to the higher values of heat balance errors corresponding to these flow patterns.

Comparison of Single Phase Heat Transfer Measurements with Correlations and Single Phase Flow Uncertainty: In this section the reliability of the experimental setup is tested by comparing the single phase heat transfer measurement taken on the setup with three standard correlations like Dittus and Boelter (1930), Ghajar and Tam (1994) and Seider and Tate (1936), inaddition to the uncertainty analysis for this single phase flow data based on Kline and McClintock (1953). For this purpose single-phase data was taken at 0^0 inclination in a Reynolds number range of 6,800 to 25,000. This measured h_{TP} values was compared against the above

correlations listed in Table 3.3. Seider and Tate (1936) was able to predict the measured data within ±10%, which is clearly shown in Figure 3.6 and also all the three correlations were able predict the data with ±15%.

Table 3.3 List of single phase heat transfer correlations

Source	Single phase heat transfer correlations
Dittus and Boelter (1930)	$Nu_L = 0.023 Re^{\frac{4}{5}} Pr^n$ *Where n = 0.4 for heating*
Ghajar and Tam (1994)	$Nu_L = 0.023 Re^{0.8} Pr^{0.385} \left(\frac{l}{D_i}\right)^{-0.0054} \left(\frac{\mu_b}{\mu_w}\right)^{0.14}$
Seider and Tate (1936)	$Nu_L = 1.86 (Re_{SL} Pr_L \frac{D_i}{l})^{\frac{1}{3}}$ (Laminar) $Nu_L = 0.023 {Re_{SL}}^{0.8} {Pr_L}^{0.4} (\frac{\mu_b}{\mu_w})^{0.14}$ (Turbulent)

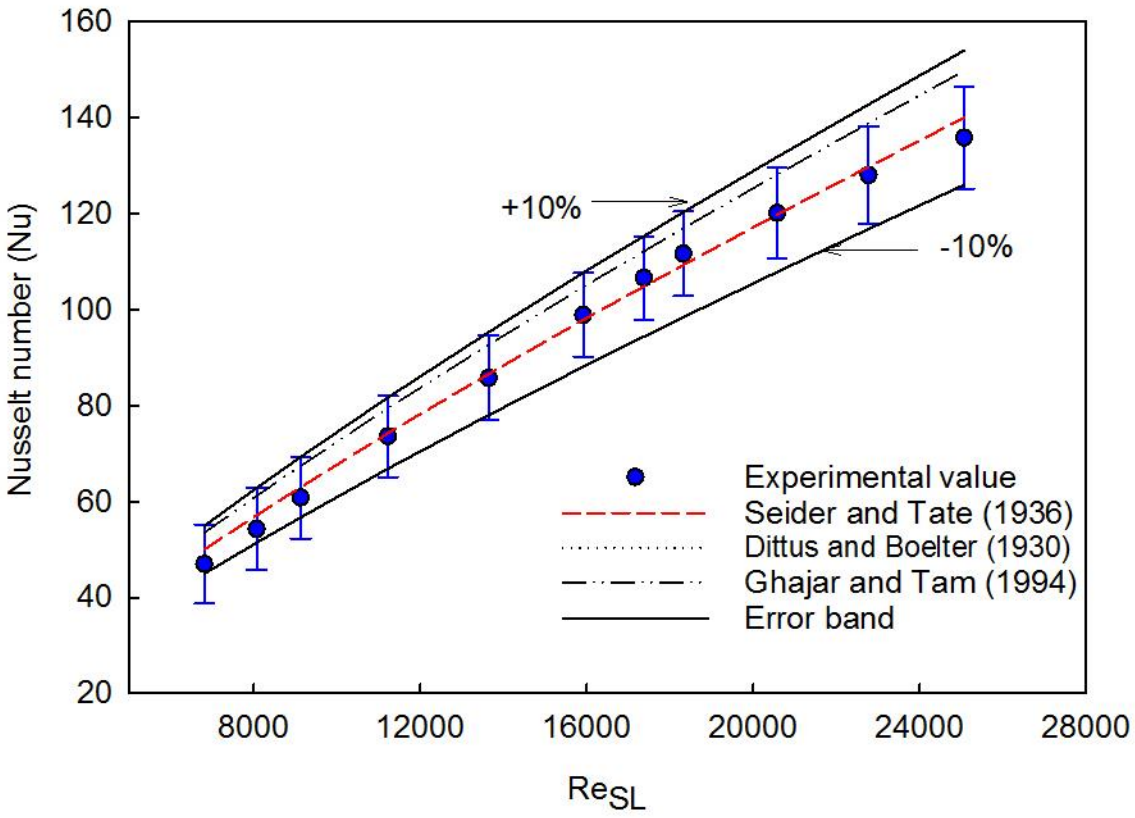

Figure 3.6 Comparison between measured and predicted values of single phase heat transfer coefficient

The absolute mean error of the single phase heat transfer coefficient was 9.58%, 7.9% and 2.35%, when Dittus and Boelter (1930), Ghajar and Tam (1994) and Seider and Tate (1936) correlations were used to calculate the mean heat transfer coefficient, respectively. The corresponding maximum errors in single phase heat transfer coefficient with respect to Dittus and Boelter (1930), Ghajar and Tam (1994) and Sider and Tate (1936) were 13.67%, 12.28% and 6.09%, respectively. The uncertainty of the populated single phase heat transfer data is calculated using Kline and McClintock (1953) uncertainty analysis for all the 11 data points and Table 3.4 shows the uncertainty associated with the measurement of single-phase heat transfer coefficient and other associated single-phase flow variables for the worst case scenario. The maximum and minimum uncertainties for the data was found to be ±10.64% and ±8.22%, respectively.

Table 3.4 Uncertainty in measured values of single phase heat transfer coefficient (worst case scenario)

Variable	Value	± Uncertainty	± % Uncertainty
Inner pipe diameter (m)	0.01252	1.27E-05	0.1
Outer pipe diameter (m)	0.0171	1.27E-05	0.07
Heat transfer length (m)	0.889	0.003175	0.31
Thermal conductivity (W/m-K)	13.438	-	-
Current (I)	582.02	5.79	1
Voltage (V)	3.95	0.0396	1
Inner wall temperature (^oC)	36.42	0.51	1.41
Heat transfer rate (W)	229961	32.51	1.34
Heat transfer coefficient (W/m^2 K)	6629.14	705.41	10.64

Comparison of Two phase Heat Transfer Measurements with Past Work: In this section, a sample of two phase flow data points for $+90^0$ are procured from the past work of Mollamahmutoglu (2012) to compare at a similar mass flow rates against the present data as shown in Figure 3.7. This comparison is performed at two similar water flow rates of 204 kg/hr and 340 kg/hr for the present study and that of Mollamahmutoglu (2012). As seen in the Figure

3.7 there was a close match between the heat transfer trends of the present work and that of Mollamahmutoglu (2012). It should also be observed that there is some deviations because of the some minute differences in water mass flow rates and also due to the change in viscosity of the water resulting from the difference in the surrounding conditions. However based on this homologous reproduction of the data by the experimental setup at similar flow rates and pipe orientations, we can conclude that the data obtained is repeatable and accurate.

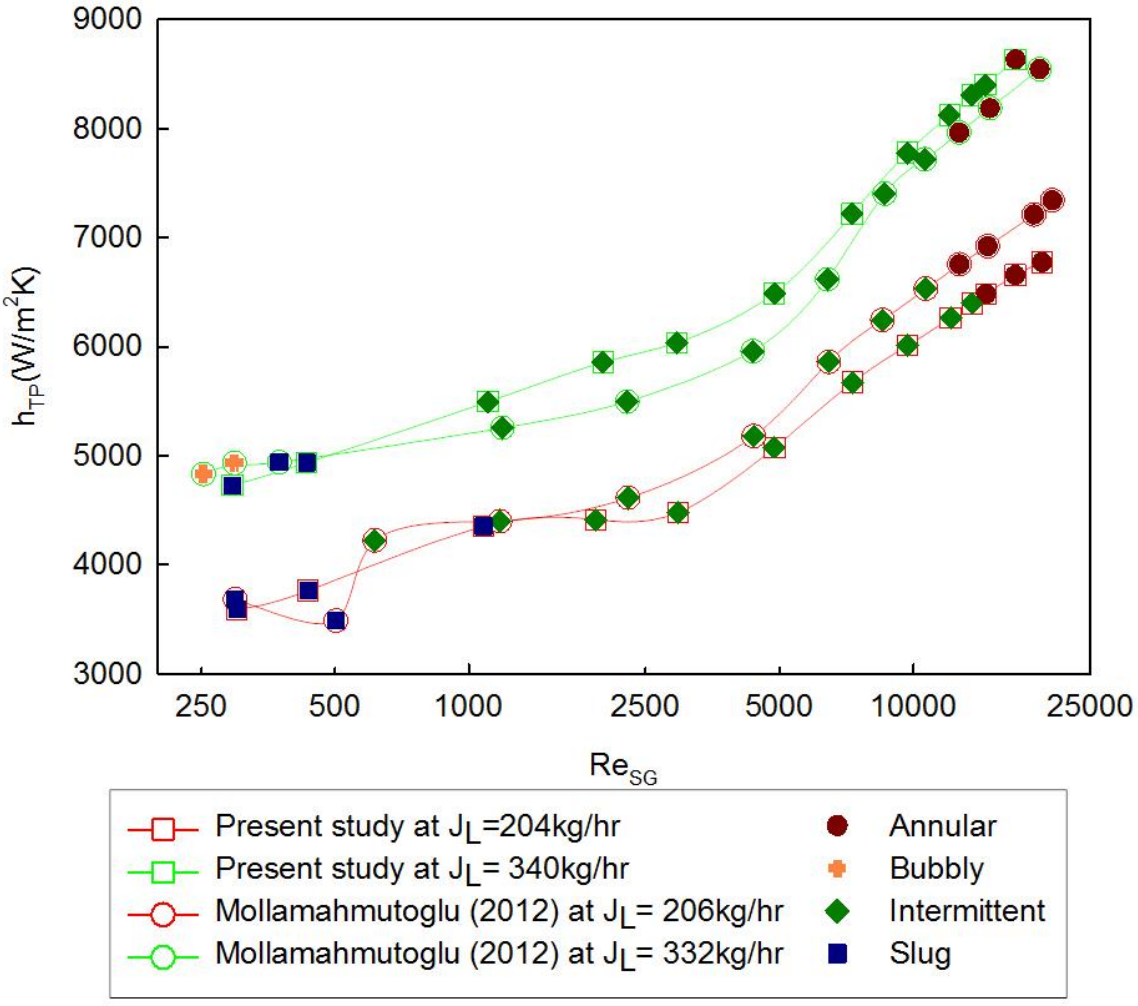

Figure 3.7 Comparison of h_{TP} obtained in present work with respect to Mollamahmutoglu (2012)

Hence, both the single phase and two phase flow data was with in the acceptable error limits with allowable uncertainty and desired repeatability. So, it can be concluded that the setup is working properly and is capable of producing accurate and reliable data.

CHAPTER IV

RESULTS AND DISCUSSION

In this chapter, a detailed analysis of the experimental results will be presented. Firstly, flow patterns and flow pattern maps available for the present study will be discussed in Section 4.1 titled “Flow Patterns and Flow Pattern Maps”. This is further divided into two subsections to show the effect of varying inertia, buoyancy and gravitational forces on flow patterns and flow pattern maps at various phase flow rates and pipe inclinations. After this various interesting trends in the heat transfer coefficient for two-phase flow are presented in Section 4.2 titled “Heat Transfer in Two-Phase Two-Component flows”. This section is divided in four subsections to discuss the effect of flow patterns, pipe orientation, pipe diameter and fluid properties on two-phase heat transfer coefficients. The final part in this Chapter comprises of analysis of various heat transfer correlations presented in Table 2.1 with respect to the present data and also with certain preselected data sets from the literature. This section is titled “Analysis of Heat Transfer Correlations Performance” and is divided into four subsections to investigate the performance of these heat transfer correlations for varying flow patterns, pipe orientations, pipe diameters and fluid combinations. Finally based on these results, the best performing heat transfer correlation that can predict the two-phase heat transfer coefficient irrespective of flow and pipe parameters mentioned earlier is identified.

4.1 Flow Patterns and Flow Pattern Maps

In two-phase two component flows the complicated interactions between the body and surface forces are driven by the density difference between the two phases and compressibility of the gas phase. These effects depending upon the fluid flow rates and pipe inclinations gives rise to a particular type of geometric distribution of the component phases called flow pattern. In addition to the distribution of the two-phases in the pipe cross section the flow pattern also regulates the diffusivity between the two phases and also the velocity of the mixture, thus having a direct effect on the void fraction, pressure drop and heat transfer. So, it is very important to review the changes in the flow pattern for establishing an idea about the variation of heat transfer for different flow parameters like pipe orientation and fluid properties. A flow pattern map is formulated by systematically coordinating the flow rates of air and water with respective flow pattern observed at that particular pipe inclination. This interpretation of various flow patterns and flow pattern map is highly qualitative in nature and is mostly subjected to the investigators perception. The present study used the flow patterns and flow pattern maps of Bhagwat (2015), who's identification of flow patterns and production of flow patterns maps were done based on the procedure suggested by Taitel and Dukler (1976). All these observations were conducted in a clear polycarbonate observation section of the current experimental setup with 12.7mm I.D. by varying the gas and liquid flow rates in a range of 0.001 to 0.2 kg/min and 1 to 12 kg/min, respectively with pipe orientation ranging from -90^0 to $+90^0$. A total of five major flow patterns called stratified, annular, intermittent, slug and bubbly are seen for $0 \leq \theta \leq +90^0$ pipe orientation range. The respective pictures of these flow patterns are given in Figure 4.1 for a pipe inclination of $+20^0$ except for stratified flow, which was only seen at 0^0 and two respective picture of the slug and intermittent flows are shown in Figure 4.1 (a) and (b) to indicate variations in the physical appearance of the flow pattern during their onset and departure to other flow patterns.

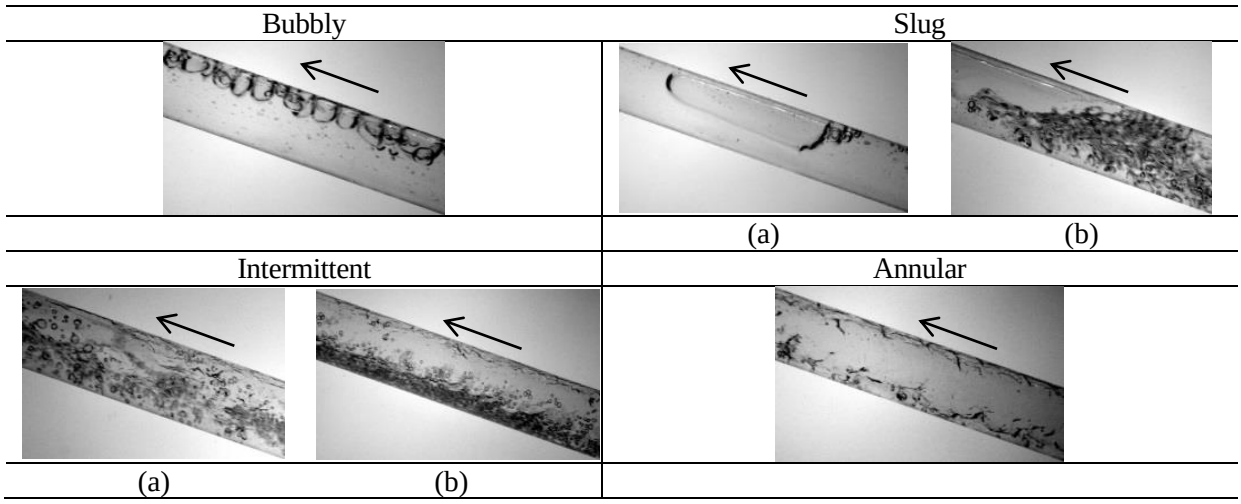

Figure 4.1: Flow patterns observed in upward inclined two phase flows (Korivi et al. (2015)).

4.1.1 Effect of Fluid Flow Rates on Flow Patterns

The occurrence of various flow patterns at different pipe inclinations is given in Figure 4.2. It can be seen that the stratified flow which occurs only in horizontal pipes for the present study typically occurs for low liquid flow rates (≤ 1.2kg/min) and low to moderate gas flow rates (≤ 0.1kg/min). This flow is characterized by separate flows of gas and liquid films with liquid film at the bottom of the pipe due to higher density. This stratified flow is transferred to slug flow as the liquid flow rate is increased because of increase in the viscous forces. The slug flow is characterized by the alternating flow of an elongated gas bubble and a liquid slug occurring at low to moderate gas (≤ 0.01kg/min) and liquid (≤ 5kg/min) flow rates consistently at all inclinations as seen from Figure 4.2.

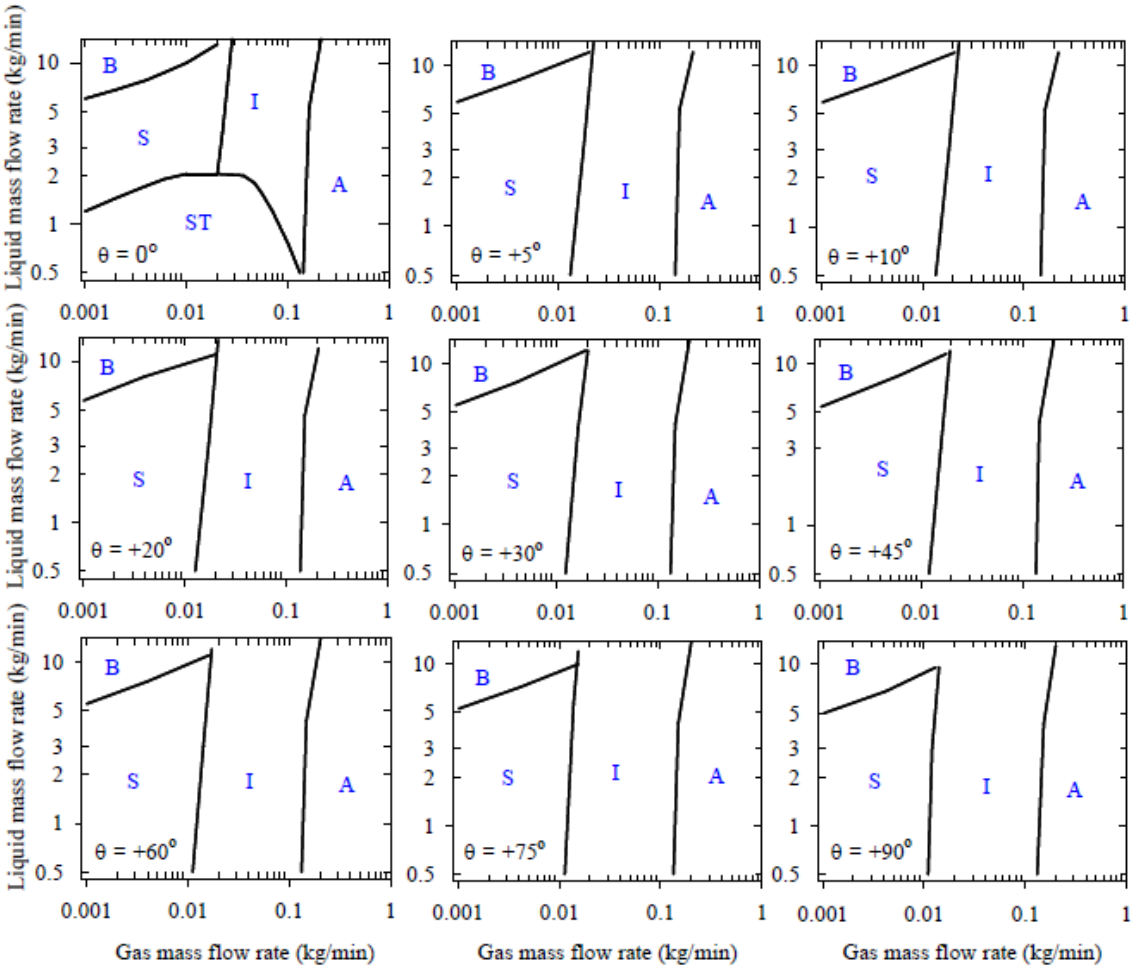

Figure 4.2: Flow pattern maps for upward inclined two phase flow (B = Bubbly, S =Slug, I = Intermittent, A = Annular, ST= Stratified) (Bhagwat (2015)).

An increase in gas and liquid flow rates act to reduce the bubble length and to aid the slug velocity. A further increase in gas flow rate (≥ 0.01kg/min) shears the elongated gas bubble to form a continuous layer of gas film in-between the liquid layers resulting in slug-wavy and wavy flows. Whereas, with further increase in the liquid flow rates(≥ 5kg/min) the viscous forces are able to overcome the surface tension forces thereby shearing the elongated bubbles into tiny bubbles resulting in bubbly flows. The intermittent flows consists of slug-wavy flows, wavy flows and annular-wavy flows, which is characterized by chaotic, pulsating and indefinite phase alignments. This flow regime generally exist at moderate gas flow rates (0.01 to 0.1 kg/min) for a given liquid flow rate and is seen at all pipe orientations as shown in Figure 4.2. With a further

increase in the gas flow rate (≥ 0.1kg/min) the wavy nature of the liquid layer surrounding the central gas flow is almost lost and annular flow regime is said to have appeared, at this point the flow is completely inertia driven. In the present discussion for the purpose of clarity the transition between the flow patterns is assumed to be quick given by a thin line as seen in Figure 4.2 but in general a more gradual transition occurs between the flow patterns over a range of gas and liquid flow rates.

4.1.2 Effect of Pipe Orientation on Flow Pattern

The effect of pipe orientation on flow pattern can be seen in Figure 4.3. It can be seen that with increase in the pipe orientation the flow regime tends toward more shear driven flow patterns. It is also observed that an increase in inclination of the pipe promotes an early slug-bubbly transition because of the increase in inertia force exerted by the liquid slug on the elongated gas bubble, which helps in disintegration of the elongated gas bubbles into tiny bubbles. The slug-intermittent transition also tends to occur at lower gas flow rates because of the increased buoyancy with respect to increased inclination. This buoyancy tends to increase the velocity of the slug and also aids the gas phase to shear through the liquid slug layer in-between the elongated bubbles, which is clearly evident at high liquid flow rates as seen in Figure 4.3.

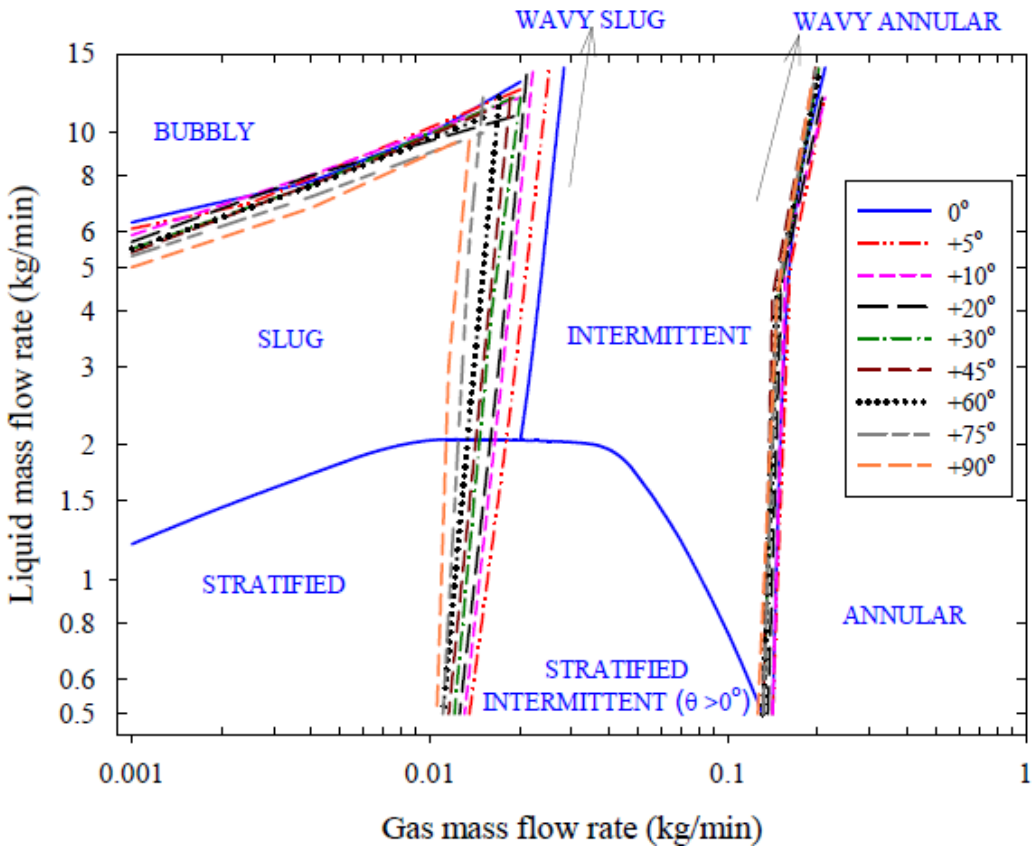

Figure 4.3: Combined flow pattern map for upward inclined pipe orientations (Bhagwat (2015)).

The transition between intermittent and annular flows regime is not effected by the pipe orientation as seen in Figure 4.3. This is due to the inertia driven nature of these flows. However, increasing the pipe orientation promotes an early annular flow regime. In total, it can be seen from Figure 4.3 that the transition from one flow pattern to other is changing in a gradual way depending upon changing the pipe orientation. Even though, the above discussed transitions and flow maps are verified with respect to various sources from the two-phase flow literature as seen in Bhagwat (2015) to be accurate, some errors might arise often from the dimensionality of the coordinates especially if these flow maps were used for other fluid combinations and pipe diameters apart from air-water flows in 12.5mm I.D pipes. It should also be noted that although the flow patterns are named the same for different pipe orientations, the physical shape or the

geometrical distribution of the phases for all the flow patterns changes with respect to pipe orientation, similar to the one shown in the Figure 4.4 for slug flow. At horizontal inclination the buoyancy force is directed to the upper wall leading to the concentration of the gas phase near the upper wall as seen in Figure 4.4 (a) for horizontal orientation and Figure 4.4 (b) at the pipe orientation of $+20^0$, where the elongated bubble is concentrated towards the upper wall surface.

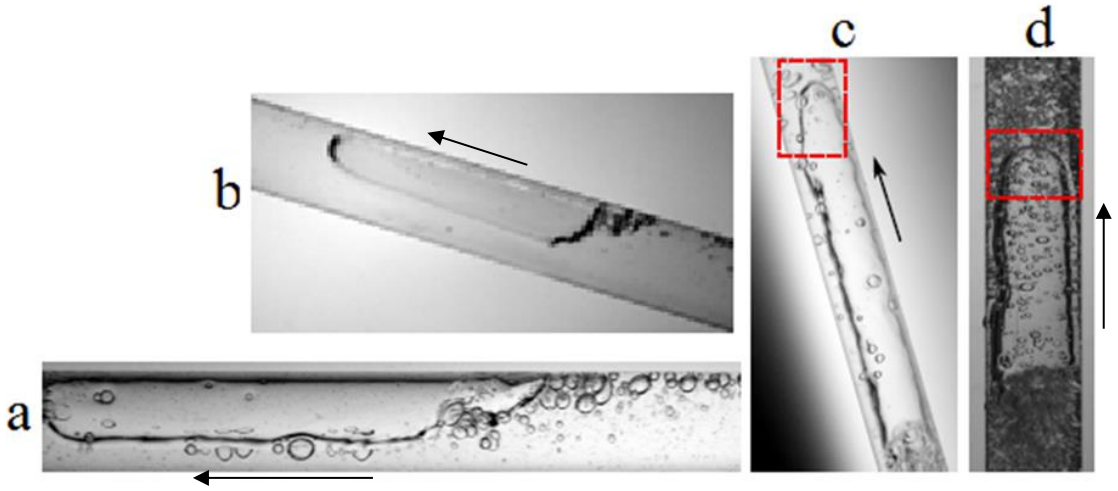

Figure 4.4: Variation of flow pattern (slug flow pattern) shape with respect to inclination.
a) At 0^0 b) At $+20^0$ c) At $+75^0$ d) At $+90^0$

On the other hand, when the pipe tends to more vertical orientation the buoyancy force tends to direct towards the flow direction allowing the flow to obtain a more axisymmetric flow distribution and aiding the gas-phase to accumulate near the center of the pipe as seen in Figure 4.4 (c) for pipe at $+75^0$ orientation and Figure 4.4 (d) for pipe at $+90^0$ vertical upward position. However, this phenomenon also tends to promote the liquid holdup. At these steeper orientations the liquid holdup is seen due to the influence of gravity and density on the fluid combination, resulting in different velocities for each fluid phase. This effect favors the lighter phase (air) to move faster than the heavier liquid phase resulting in the holdup of liquid near to the wall due to the slippage between both of these phases. This holdup of near wall liquid is also called liquid holdup.

4.2 Heat Transfer in Two-Phase Two-Component Flows

The heat transfer in two-phase flows is found to be effected by many factors like geometric distribution of fluid phases, pipe orientation, pipe geometry and fluid properties. The below discussion uses the data from the present study and also from the data reported in two-phase flow literature in Chapter 2.1 to analyze the behavior of the two-phase flows in view of the above mentioned parameters. Different trends in the heat transfer coefficient for varying flow rates, pipe orientations, tube diameters and fluid combinations are identified and scrutinized in view of the changing physical interactions between the body and surface forces for both phases. For this purpose measurements of two phase flow heat transfer coefficient and other required flow parameters were conducted for pipe orientations of 0^0, $+5^0$, $+10^0$, $+15^0$, $+20^0$, $+30^0$, $+45^0$, $+60^0$, $+75^0$ and $+90^0$. The gas and liquid mass flow rates (phase superficial Reynolds numbers) are varied in a range of 0.003 to 0.2kg/min ($290 \leq Re_{SG} \leq 19000$) and 1.36 to 9.1kg/min ($1970 \leq Re_{SL} \leq 13200$) to cover all the flow patterns (stratified, slug, bubbly, intermittent and annular) at all the above specified orientations.

4.2.1 Effect of Phase Flow Rates and Flow Patterns on h_{TP}

Distinct heat transfer trends are associated to each flow pattern in correspondence to the unique geometrical distribution of fluid phases, which are caused due to the varying phase flow rates. These trends are also found to be influenced by the pipe orientation. So, it is necessary to categorize the experimental data into comparable superficial liquid and gas Reynolds numbers at each orientation as shown in Figures 4.5, 4.6 and 4.7. Some of these trends in the two-phase heat transfer coefficient are only specific to a particular range of pipe inclination. So, in-order to facilitate a detailed analysis, the data is further grouped into horizontal and near horizontal inclinations ($0^0 \leq \theta \leq +30^0$), mid-range pipe inclinations ($+30^0 < \theta \leq +60^0$) and vertical and near vertical pipe inclinations ($+60^0 < \theta \leq +90^0$) corresponding to Figure 4.5, Figure 4.6 and Figure 4.7, respectively.

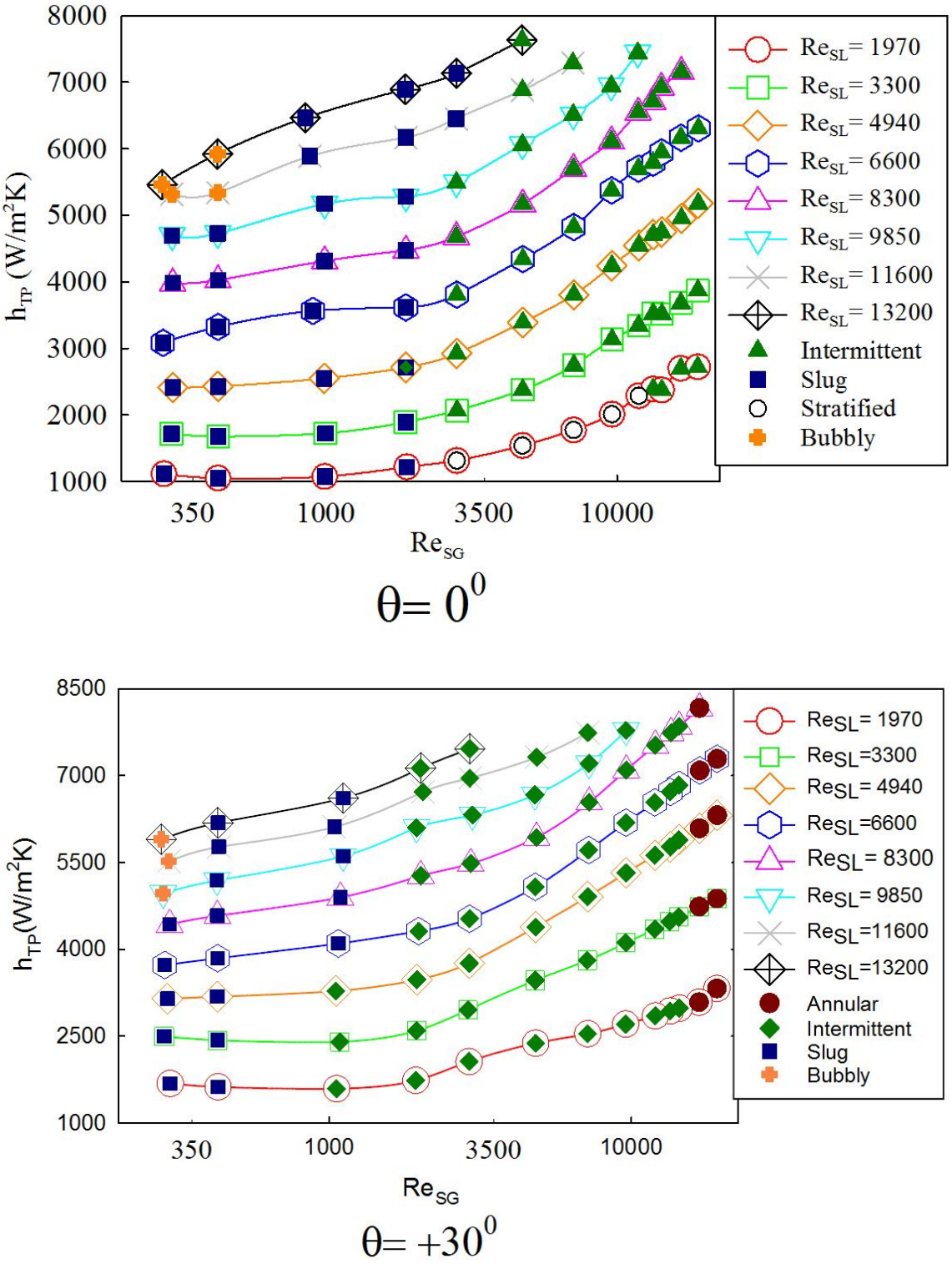

Figure 4.5 Variation of h_{TP} with respect to changing Re_{SL} and Re_{SG} for horizontal and near-horizontal oriented two phase flows ($0^0 \leq \theta \leq +30^0$)

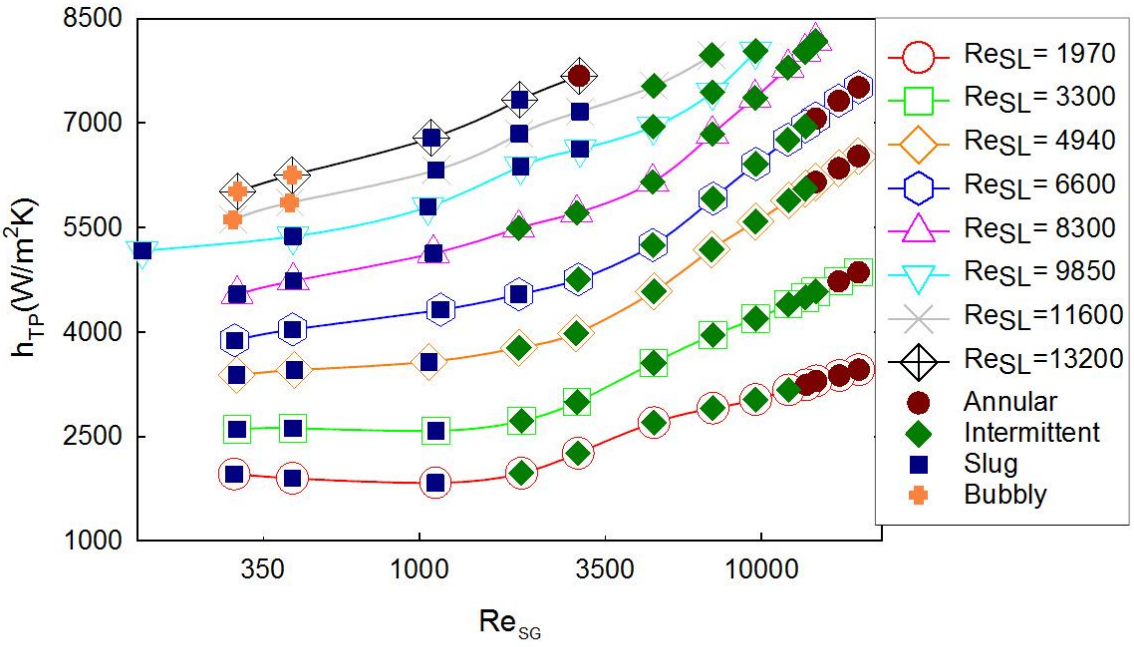

$\theta = +45^0$

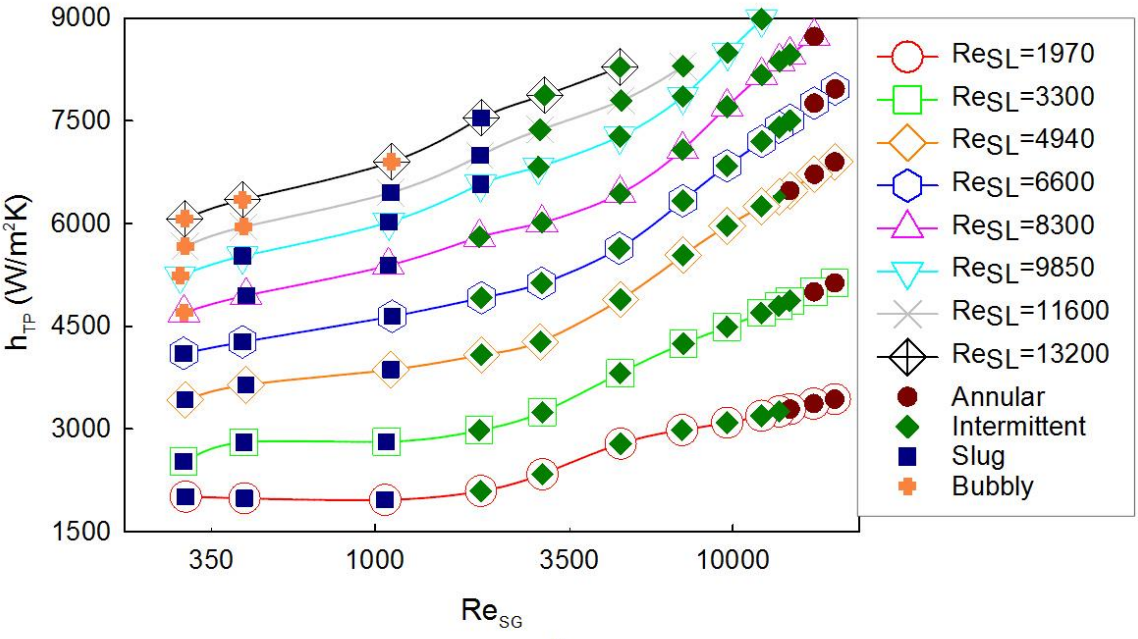

$\theta = +60^0$

Figure 4.6 Variation of h_{TP} with respect to changing Re_{SL} and Re_{SG} for mid-range inclined two phase flows ($+30^0<\theta\leq+60^0$)

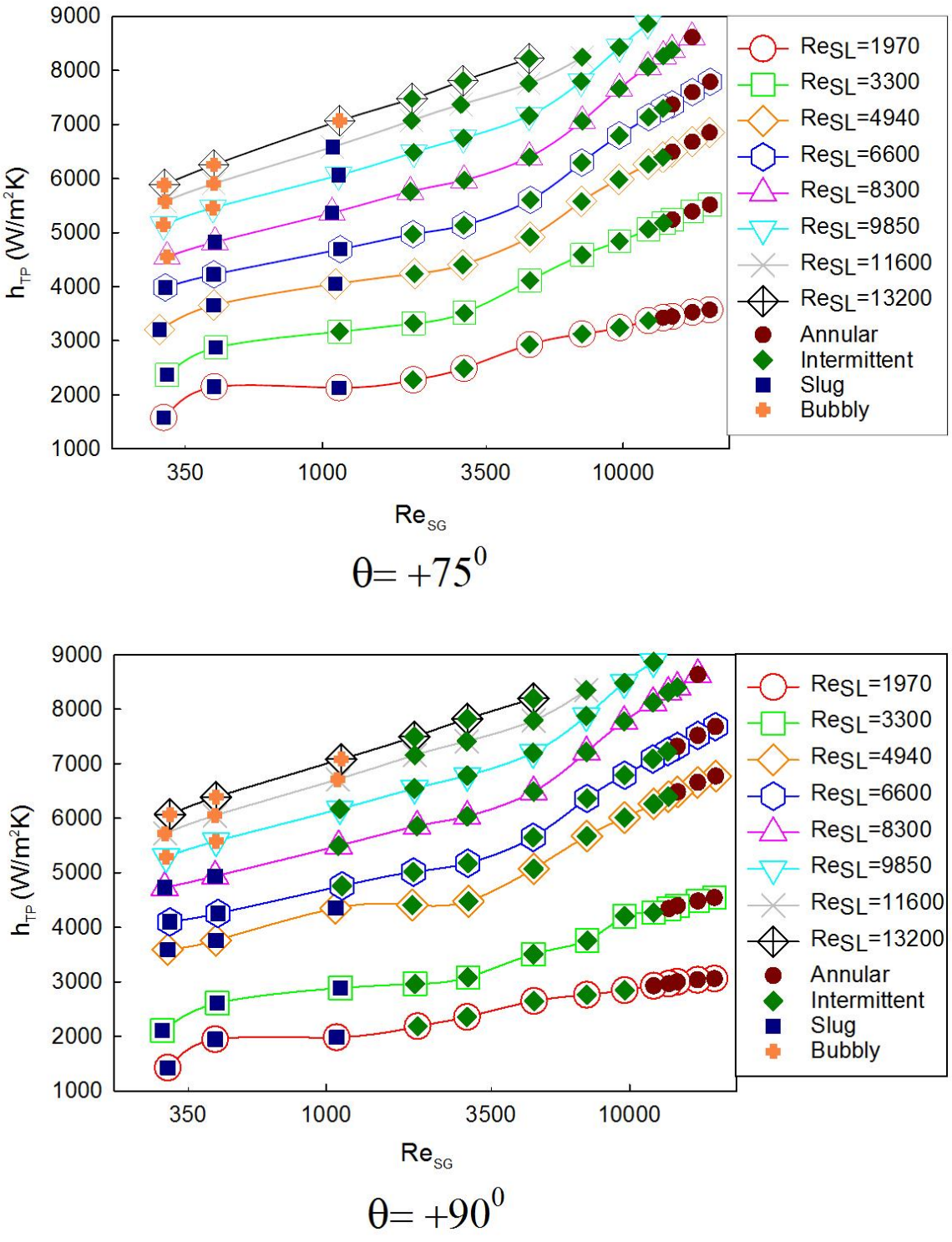

Figure 4.7 Variation of h_{TP} with changing Re_{SL} and Re_{SG} in vertical and near-vertical inclined two phase flows ($+60^0<\theta\leq+90^0$)

It can be seen at low liquid flow rates (Re_{SL}≤6600) and low gas flow rates for horizontal and mid-range pipe inclinations from Figures 4.5 and 4.6, that the increase in the two phase heat transfer coefficient (h_{TP}) is insensitive to the increase in the gas flow rates. This is seen from low to moderate gas flow rates (Re_{SG}≤2000) in the above mentioned range of liquid flow rates and pipe inclinations. On the other hand in the same range of gas flow rates (Re_{SG}≤2000) and liquid flow rates (Re_{SL}≤6600) for vertical and near vertical pipe inclinations there is a steep increase in the h_{TP} with respect to the gas flow rate, which can be clearly seen from Figure 4.7. It should be noticed that all the data points pertaining to this region of Re_{SG} and Re_{SL} are of slug flow regime and a few with intermittent (slug-wavy) flow pattern, which results in a buoyancy driven flows. In horizontal and near horizontal and mid-range pipe inclinations for slug flows the continuity is maintained by a partial flow of the liquid film surrounding the gas slug in downward direction, which counters the rise in local velocity of the liquid phase and hence the increase in heat transfer coefficient. It should also be noted that this flow regime at this pipe orientation is associated with weak buoyancy force which is directed towards the upper wall of the pipe. Whereas, for flows in vertical and near vertical pipe inclinations the increase in the velocity of the slug flow due to the buoyancy force that is directed in the flow direction and an increase in the effective exposed area of the pipe wall to liquid phase due to axisymmetric nature of the slug flow tends to dominate the reduction in the heat transfer caused by the downward flowing film surrounding the gas slug, hence resulting in an increase in the h_{TP} with respect to the gas flow rate, which can be clearly seen for high liquid flow rates(Re_{SL}≥4940). At all the inclinations in the range of low gas flow rates(Re_{SG}≤2000) a consistent increase in heat transfer coefficient is noted with respect to increase in the liquid flow rate for a given gas flow rate but at varying trends depending on the flow pattern as seen from Figures 4.5, 4.6 and 4.7. The flow patterns observed in this range are slug, bubbly and intermittent (slug-wavy), which can be noted from the above mentioned figures. The h_{TP} increased consistently in slug and intermittent (slug-wavy) flow pattern with increasing liquid flow rates for all the inclinations but this rise is decreased as the flow pattern is changed from

slug to bubbly at high liquid flow rates (Re_{SL}≥9000), which is noticed in all the Figures 4.5, 4.6 and 4.7. This is due to the fact that the slug flow offers more liquid phase to contact the pipe wall than bubbly flow pattern throughout which the gas phase is dispersed as tiny bubbles.

As the gas flow rate is increased further more to Re_{SG}≥2000 the slug flow pattern was transferred to intermittent (slug-wavy) flow pattern at all inclinations as seen in Figures 4.5, 4.6 and 4.7. In this region the elongated gas bubble shear the liquid slug film in-between them to form a continuous layer of gas film causing occasionally elongated, aerated and distorted gas pockets flowing through the pipe and this phenomenon helps to expose more liquid phase towards the pipe wall due to which there is a gradual increase in h_{TP} with respect to rise in Re_{SG}. This same trend is seen till the on-set of wavy-annular transition flow region at all pipe orientations. The gradual rise in h_{TP} is transferred to rapid increase in h_{TP} with steep slopes as the gas flow rate is increased even further to Re_{SG}≥9000 as seen in Figures 4.5, 4.6 and 4.7. In this range of superficial gas Reynolds numbers the flow distribution is transferred from intermittent to annular flow regimes. A sweeping action of disturbance waves at the gas-liquid interface with amplitude large enough to momentarily bridge the entire pipe cross section characterizes this onset of annular flow regime and this annular flow is credited with the largest interfacial area compared to any other flow pattern. These effects also promote the vigorous mixing and churn of the two phases in addition to adding more liquid-wall interfacial area at a given flow rate and consequently resulting in an increased heat transfer. This trend of increase in the heat transfer for intermittent and annular flows is not effected by the liquid flow rate as seen in Figure 4.5 for horizontal and near horizontal flows. But on the other hand, for mid-range and vertical and near vertical pipe inclinations at Re_{SL}≤4000 and Re_{SG}≥9000 this trend of steep increase in h_{TP} for annular flows is absent as shown in Figures 4.6 and 4.7, this is due to the liquid hold up and flow reversal phenomenon that counter the rise in h_{TP}, as suggested from our previously measured pressure drop data for the same setup. However, at higher liquid flow rates (Re_{SL}≥5000) in this gas flow rate range (Re_{SG}≥5000) for mid-range and vertical and near-vertical pipe

inclinations the trends exhibited by intermittent and annular flows were very similar to the trends exhibited by horizontal and near-horizontal flows in the same range of Re_{SL} and Re_{SG}. In general, we can conclude that the effect of flow pattern and phase flow rates on two-phase heat transfer is highly appreciable but this phenomenon for buoyancy dominated flows is dependent on the pipe orientation, whereas as for inertia driven flows this variation of h_{TP} will more or less remain the same irrespective of pipe inclination. It should be noted that in total the h_{TP} increases with increase in gas and liquid flow rates. Also, for intermittent and annular flows at high liquid flow rates (Re_{SL}≥5000) no significant effect of pipe orientation on the overall trends of h_{TP} is observed.

4.2.2 Effect of Pipe Orientation on h_{TP}

As seen from the discussion in Section 4.2.1 the heat transfer in two phase flows is not only effected by the flow pattern but also by the pipe orientation. A preliminary analysis of the measured two phase heat transfer coefficient shows that the effect of pipe orientation on the two-phase flow can even be very significant due to the change in the physical structure of the two-phase flow patterns as discussed in Section 4.1. So, in-order to clearly analyze the effect of pipe inclination on two-phase flows the data is grouped into various categories of superficial liquid Reynolds numbers and superficial gas Reynolds numbers with respect to changing pipe orientations as shown in Figures 4.8 and 4.9. To identify the complicated trends of varying h_{TP} and for the purpose of lucid presentation the data measured is categorized into high, medium and low liquid phase flow ranges corresponding to Re_{SL}≥9850, 3300<Re_{SL}>9850 and Re_{SL}≤3300 and high, medium and low gas phase flow rate ranges corresponding to Re_{SG}≥4800, 425<Re_{SG}>4800 and Re_{SG}≤425, respectively. Figure 4.8 (a), (b) and (c) corresponds to low, medium and high liquid flow rate data and similarly Figure 4.9 (a), (b) and (c) corresponding to low, medium and high gas flow rate data.

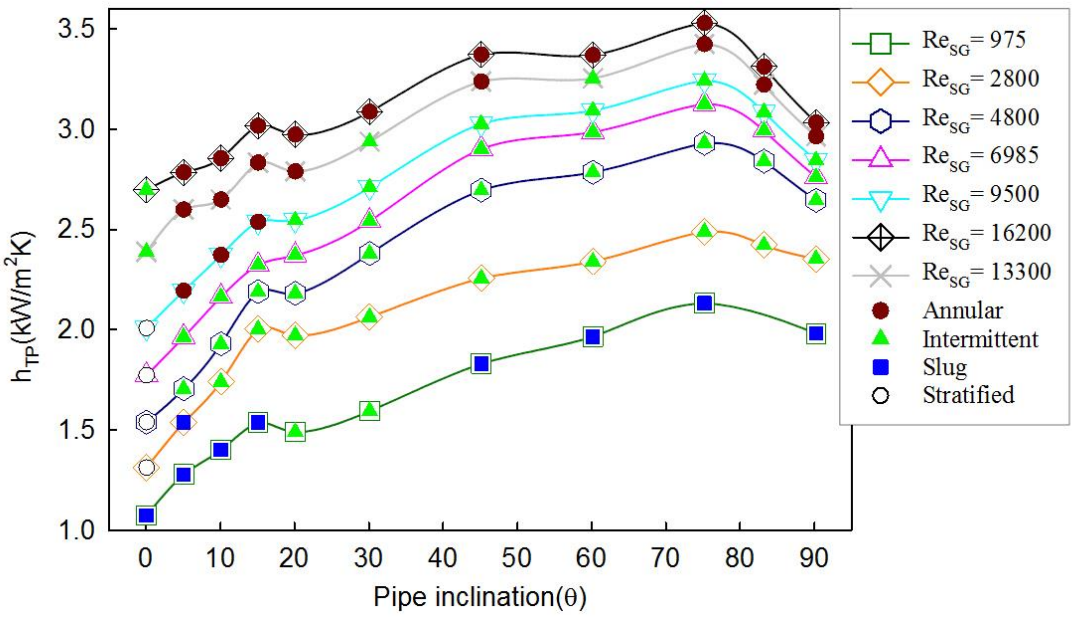

(a) At low liquid flow rate (Re_{SL}= 1970)

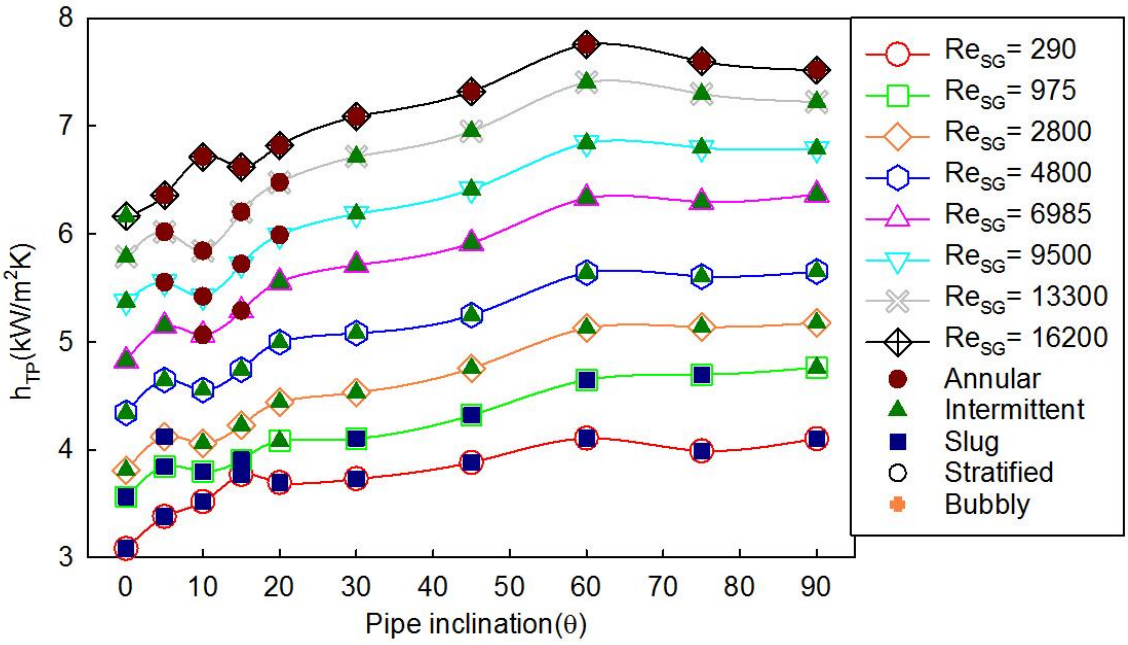

(b) At medium liquid flow rate (Re_{SL}= 6600)

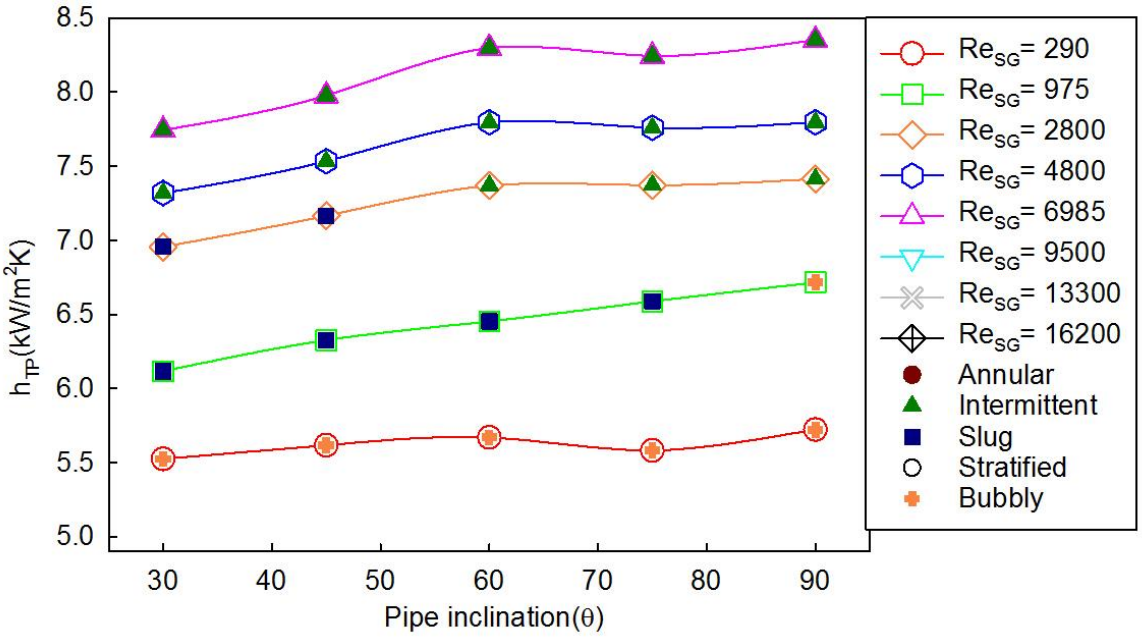

(c) At high liquid flow rate (Re_{SL}= 11600)

Figure 4.8 Effect of pipe orientation on h_{TP} for fixed Re_{SL} and varying Re_{SG}

The change in the heat transfer coefficient at varying pipe inclinations for the same fluid combination (air-water mixture) is mainly due to the changing interactions between the gravitational and buoyancy forces that promote the inertia force with respect to increasing pipe orientation. For low liquid flow rates(Re_{SL}≤3300) at all gas flow rates as seen in Figure 4.8(a) for a sample of Re_{SL}= 1970, the two-phase heat transfer coefficient tends to increase till around $+75^0$ and then starts to decrease from $+75^0$ to $+90^0$. This particular trend is seen at all flow rates in this range and can also be noticed at Re_{SL}=3300 from Figure 4.9. This is due to the fact that as the inclination increases the thickness of the liquid layer on the upper wall gradually increases as shown in Figure 4.4 there by increasing the heat transfer coefficient. This axisymmetric flow distribution is caused by the buoyancy and cohesion forces that tend to drive the gas phase towards the centerline of the pipe. On the contrary, this increase in the pipe orientation also opposes the fluid motion and promotes liquid holdup due to the gravitational force, consequently decreasing the heat transfer coefficient. So, we can conclude

that the relative magnitude of buoyancy and gravitational forces aid and oppose the motion of gas phase and hence the heat transfer in two phase mixture. This balance between the above mentioned effects shape the variation of h_{TP} with respect to pipe inclination for various flow rates accordingly. For this particular range of low liquid flow rates the rise in h_{TP} caused by the increase in axisymmetric flow distribution promoted by gravity and buoyancy forces dominate the liquid holdup induced by the increasing gravitational component till $+75^0$, thus showing an increase in h_{TP} with respect to pipe inclination as seen in Figure 4.8(a). But after $+75^0$ the liquid holdup gains an upper hand consequently decreasing the h_{TP} till $+90^0$. At medium liquid flow rates there is more gradual increase in the h_{TP} till $+60^0$ and at high liquid flow rates there is even more gradual increase in the h_{TP} till $+60^0$ as seen in Figures 4.8 (b) and (c) respectively, this increase is due to the same reason given for low liquid flow rates but the decrease in the nature of increments of h_{TP} is due to the addition of gas phase to already chaotic and inertia dominated flows, because of high liquid content in the flow geometry. But the decrease in h_{TP} observed at low liquid flow rates from $+75^0$ to $+90^0$ is not seen at medium and high liquid flow rates as seen in Figures 4.8(b) and (c) because at low liquid flow rates the fluid mixture has low liquid content and hence low inertia, which is unable to promote enough diffusivity of both phases to overcome the liquid holdup caused by the increasing pipe orientation and hence resulting in a decrease in h_{TP} at vertical orientation compared to near vertical orientations. However for medium and high liquid flow rates there is a significant liquid phase in the flow enough to cause sufficient inertia force to promote the dispersion of the two-phases and hence reducing the liquid holdup, there by maintaining the h_{TP} constant in the vicinity of vertical orientation and near vertical orientations. This effect of increased tendency to attain more inertia driven or diffused flow patterns with respect to increase in inclination and liquid mass flow rate is clearly seen in Figure 4.3 and also at Re_{SG}= 975 from Figures 4.8 (b) and (c), where the slug flow pattern is changed to slug-wavy flow pattern for medium flow rates and to bubbly for high liquid flow rates as the inclination is increased from $+75^0$ to $+90^0$. These observations are consistent with Spedding and Chen (1984) and Bhagwat (2015), who suggested that in comparison to vertical upward flow, the flow structure

(liquid and gas phase distribution) across the pipe cross section in near vertical inclined pipes exhibits anisotropy, which favors additional liquid holdup.

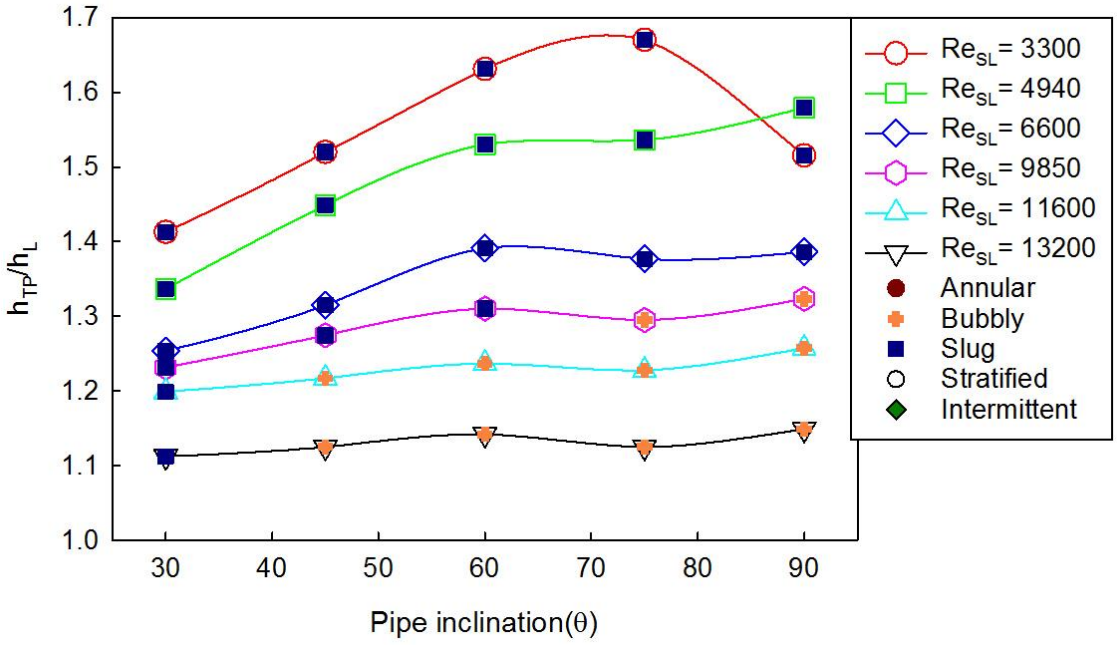

(a)At low gas flow rate (Re_{SG}= 425)

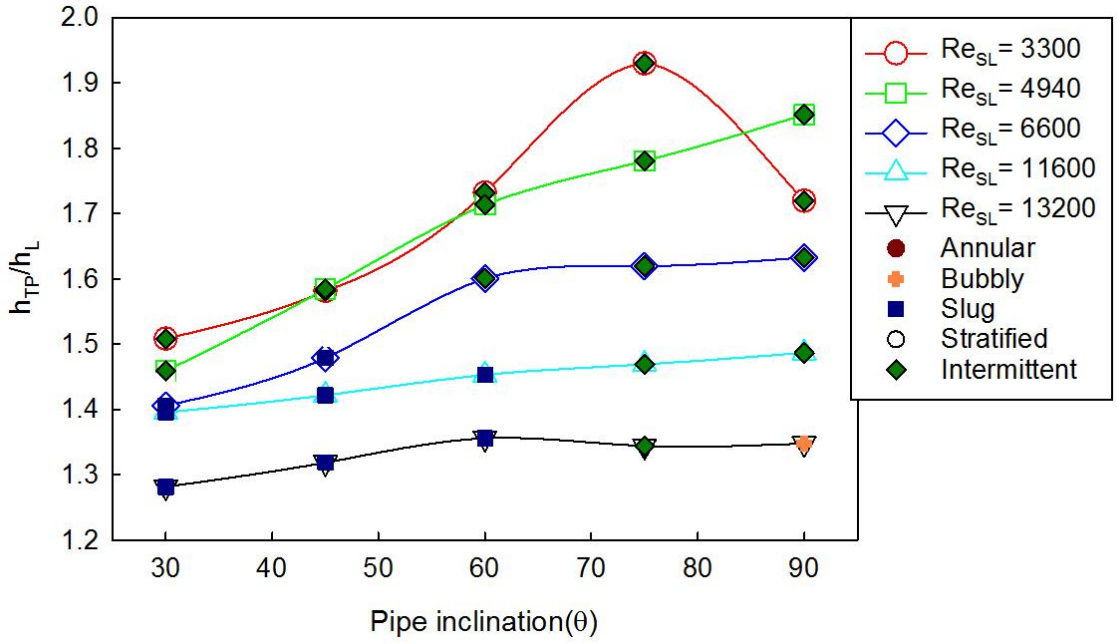

(b) At medium gas flow rate (Re_{SG}= 1900)

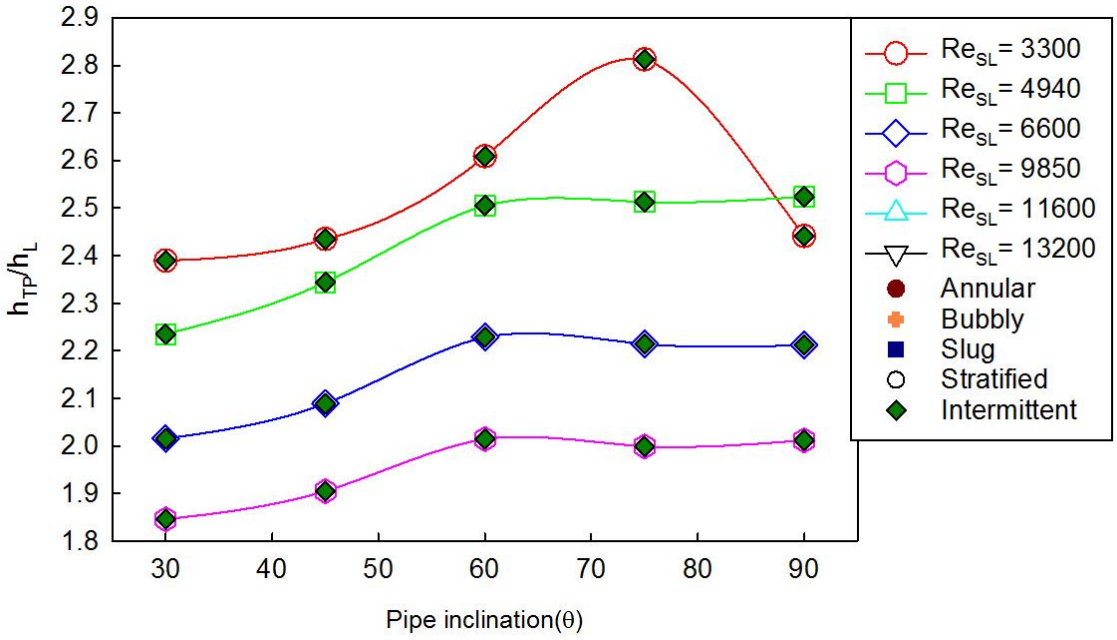

(c) At high gas flow rate (Re_{SG}= 9500)

Figure 4.9 Ratio of two phase to single phase heat transfer coefficient for varying pipe orientations at given Re_{SG} and varying Re_{SL}

Figures 4.9 (a), (b) and (c) give variation of ratio of two phase heat transfer coefficient to single phase heat transfer coefficient (h_{TP}/h_L) with respect to pipe inclinations for low, medium and high gas flow rates, respectively. The single phase heat transfer coefficient was measured in the same setup for that particular superficial liquid Reynolds number at horizontal orientation and can be obtained from Figure 3.6, however the uncertainty associated with these measurements should also be considered. As seen in Figure 4.9 the ratio of h_{TP}/h_L is lowest for low gas flow rates and tends to increase with increasing gas flow rate for all liquid flow rates and flow patterns. The reduction in h_{TP}/h_L at $+90^0$ for low liquid flow rates due to liquid holdup is also observed at all gas flow rates, which corresponds to Figure 4.8 (a). For low gas flow rates (bubbly and slug flow regime) the rise in h_{TP}/h_L with respect to inclination is rapidly high only for low liquid flow rates and at high and medium liquid flow rates this increase is almost negligible as seen in Figure 4.9 (a). Whereas at medium and high gas flow rates, where the flow mostly comprises of intermittent and annular flows the increase in h_{TP}/h_L with respect to inclination is clearly seen even for medium and high liquid flow

rates. This increment in the h_{TP} is following the same trend for all liquid flow rates in this range except for low liquid flow rates as seen from Figures 4.8 (b) and (c). In these medium and high liquid flow rates the change in h_{TP} noted as pipe inclination is changed from $+75^0$ to $+90^0$ is negligible as seen from Figure 4.9, which is also seen in Figures 4.8 (b) and (c) for the same reason of increased dispersion of gas phase due to increase in inertia forces. This phenomenon reduces the liquid holdup has mentioned earlier. This is clearly seen at Re_{SL}=13200 from Figure 4.9 (b) as pipe inclination is increased from $+75^0$ to $+90^0$, where the flow pattern changes from slug-wavy to bubbly. However in-order to verify this phenomenon, repeated experiments and flow visualization should be conducted at near vertical and vertical orientations. In total we can conclude that the effect of pipe orientation is appreciable at low liquid and low gas flow rates. Whereas this influence of pipe inclination on two-phase heat transfer coefficient tends to diminish with increasing superficial liquid Reynolds number. These observations match with the conclusions of Tang and Ghajar (2007) for 27.9mm I.D. stainless steel pipe, who conducted experiments in the range of 0^0 to $+7^0$ pipe inclinations.

4.2.3 Effect of Pipe Diameter on h_{TP}

It is seen that the effect of pipe orientation tends to diminish at high liquid flow rates ($Re_{SL}\geq$9850) but these trends are noticed for 12.5mm I.D steel pipe. So, it is interesting to know if a change in the pipe diameter would affect the h_{TP} at these ranges of superficial liquid Reynolds numbers. So, to examine the effect pipe diameter on h_{TP}, two-phase flow data of Tang and Ghajar (2007) at 27.9mm I.D. pipe and the present data for 12.5mm I.D. pipe are used as shown in Figure 4.10. This data was collected at a Re_{SL} around 9200 for the pipe orientation of $+5^0$ using air-water as a fluid combination.

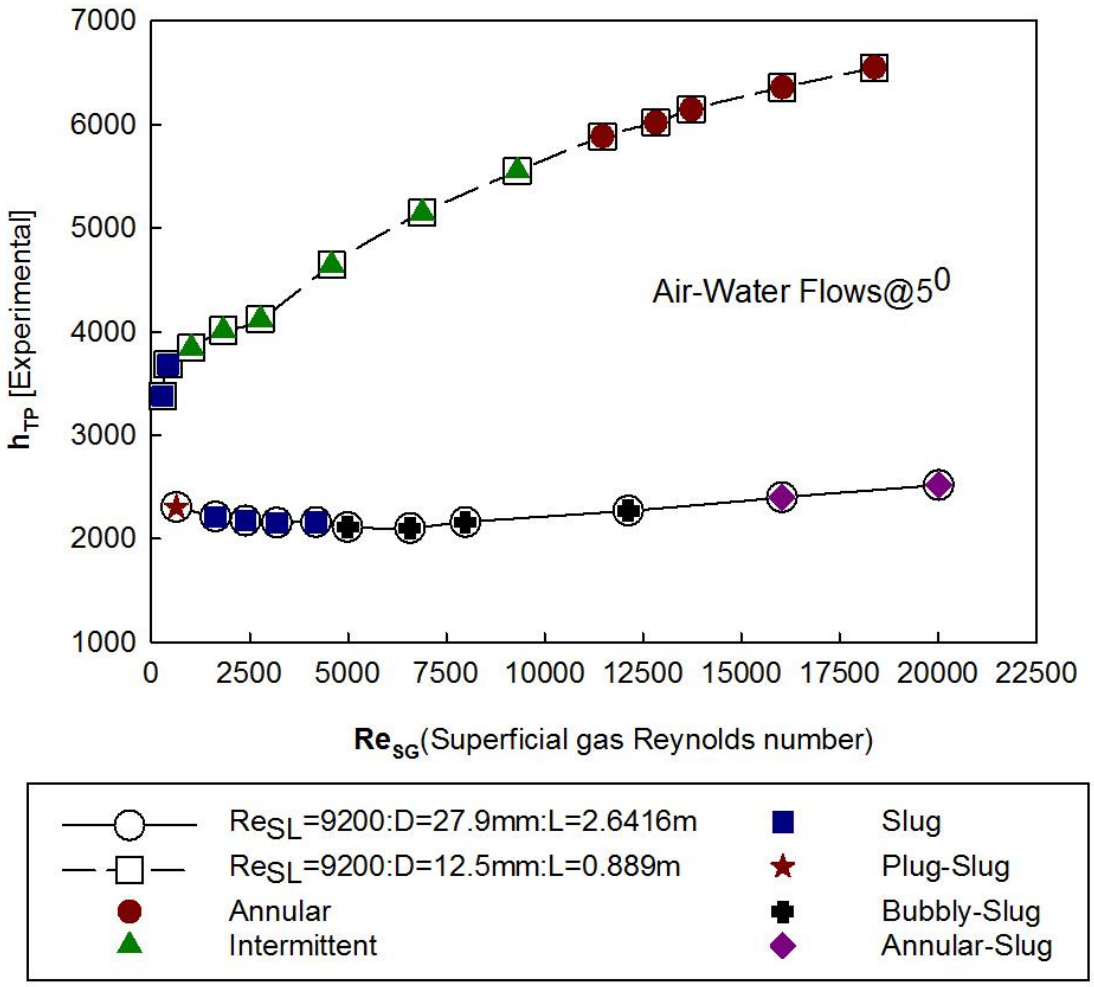

Figure 4.10 Variation of h_{TP} with respect to Re_{SG} for pipes with different diameter

It can be noticed from Figure 4.10 that similar to the single phase flows, two-phase flow heat transfer coefficient is also inversely proportional to the pipe diameter for both buoyancy driven flows (slug, slug-wavy) and inertia driven flows (wavy-annular, annular). It can also be seen from Figure 4.10 that the effect of pipe diameter is significantly large in inertia driven flows, which comprises of annular and wavy-annular flow regimes compared to buoyancy driven flows that comprises of slug and slug-wavy flow regimes. This reduction in h_{TP} for 27.9mm I.D. pipe is due to the increase in cross sectional area available to the flow, which reduces the velocity of the mixture and hence conversely effecting the heat transfer. This reduction in velocity of the mixture

can be seen from the delayed transmission of the flow structure towards more inertia driven flow patterns. This can be seen from Figure 4.10, where at Re_{SG}=600 the 27.8mm diameter pipe exhibits plug-slug flows, which transmits to slug flow that is shown till Re_{SG}=5000, from where the flow regime transfers to slug-wavy intermittent flows. Whereas, for 12.5mm I.D. pipe starts with slug flows shown only till Re_{SG}=500, from where it transfers to intermittent flows and finally to annular flows at around Re_{SG}=9500.

4.2.4 Effect of Fluid Properties on h_{TP}

The effect of gas density and mixture velocity on h_{TP} are seen in Section 4.2.1. Apart from these two factors liquid viscosity and thermal conductivity also plays a major role in influencing the phenomenon of heat transfer for two-phase flows. To analyze the effect of these liquid properties on heat transfer coefficient, data from Sujumnog (1998) for vertically upward air-glycerine (59%)+water (41%) flows in 11.68mm I.D. pipe is used at corresponding superficial liquid Reynolds numbers against the air-water data from the present study in 12.5mm I.D. pipe at the same vertical upward orientation as shown in Figure 4.11. This comparison is presented for both fluid combinations at low and high superficial liquid Reynolds numbers of 3400 and 7600, respectively as shown in Figures 4.11 (a) and (b).

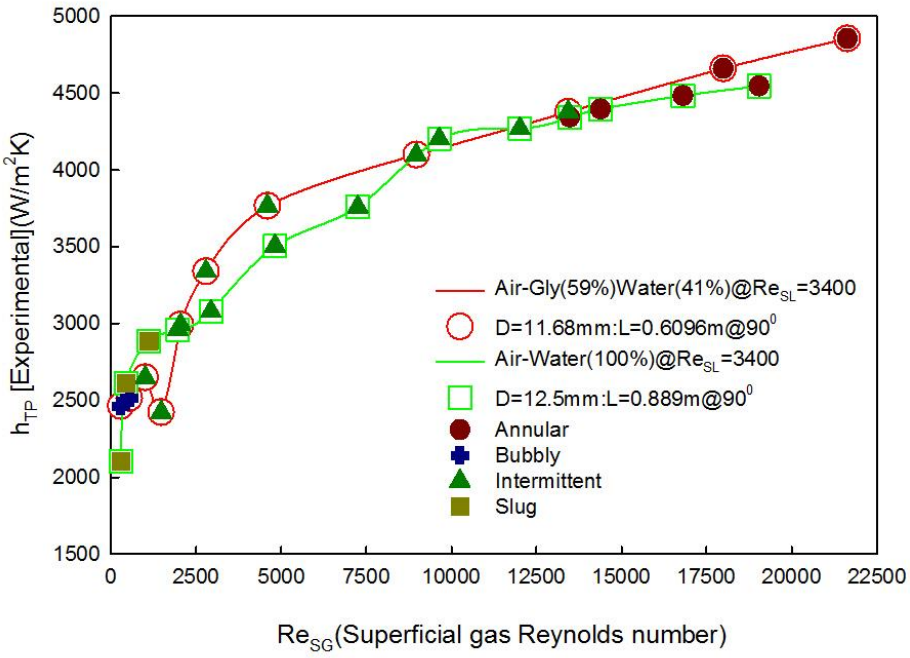

(a) At low liquid flow rate (Re_{SL}= 3400)

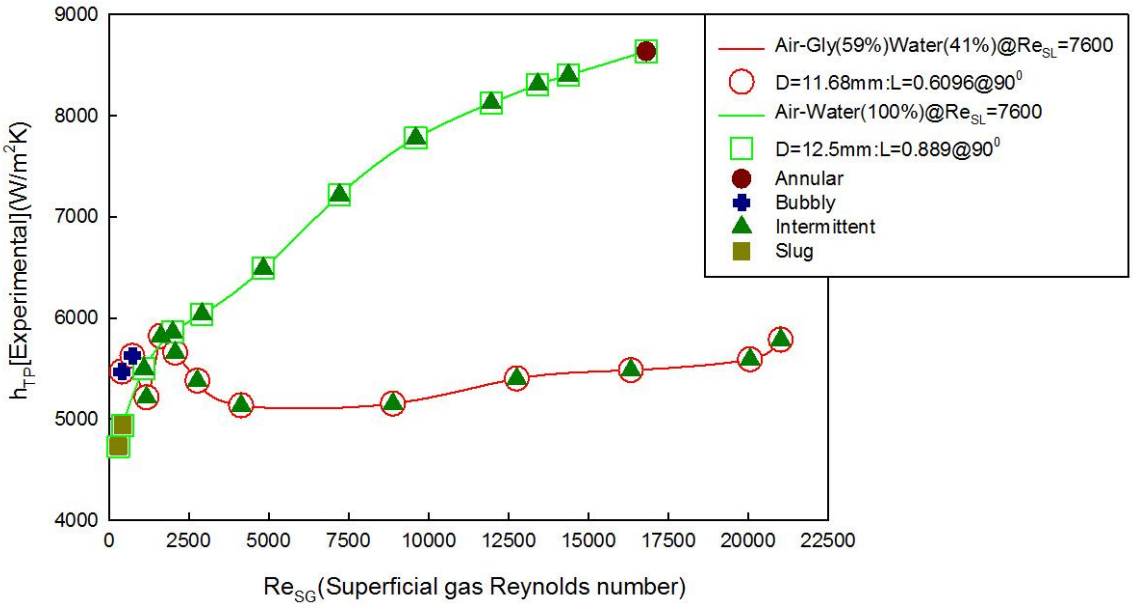

(b) At high liquid flow rate (Re_{SL}= 7600)

Figure 4.11 Variation of h_{TP} with respect to Re_{SG} for air-glycerine (59%) +water (41%) and air-water flows

It should be noted that both fluid combinations are flowing in comparable pipes with almost same diameter and also has almost same surface tension ($\sigma_{glycerine\ (59\%)\ +water\ (41\%)}$ =0.068 N/m and σ_{Water}=0.072 N/m). The viscosity, thermal conductivity for glycerine (59%) +water (41%) and water are given to be 9.8 x 10^{-3}Pa-s, 0.385 W/m.K and 8.90 x 10^{-4}Pa-s, 0.602 W/m.K respectively. At low superficial liquid Reynolds numbers as shown in Figure 4.11 (a) the variation of h_{TP} with respect to Re_{SG} is mostly identical for both fluid combinations, even though glycerine(59%)+water(41%) has only half the value of thermal conductivity of water and ten times higher viscosity than water. This is because of the fact that at lower superficial liquid Reynolds numbers the net increase in the heat transfer is mostly due to the increase in the velocity of the mixture by the gas-phase because of lower amounts of liquid-phase in the pipe. However, at higher superficial liquid Reynolds numbers the heat transfer is also influenced by the net amount of liquid phase in the pipe mostly by the near wall fluid that tends to play a major role in this phenomenon. It should be observed that glycerine (59%) +water (41%) have higher viscosity and lower thermal conductivity compared to water and at vertical orientations both walls are completely covered by the liquid phase due the induced axisymmetric flow distribution of two phase flows and because of these reasons there is a significant difference in the h_{TP} with increasing superficial gas Reynolds number for these high liquid flow rates as seen in Figure 4.11 (b). This increase in viscosity tends to promote a more laminar nature in the flow, there by showing a constant h_{TP} with respect to increasing Re_{SG} for air-glycerine(59%)+water(41%) at high liquid superficial gas Reynolds numbers as shown in Figure 4.11 (b), which is very similar to the observations given by Vijay (1978) and Sujumnong (1998).

4.3 Analysis of Heat Transfer Correlations Performance

As mentioned earlier in Section 2.2, the two-phase literature provides several correlations to predict non-boiling two-phase heat transfer coefficient. However, these correlations are mostly developed and validated against data in horizontal and vertical upward pipe orientations. The accuracy for upward inclined two-phase flows, pipes of variable diameters and different fluid combinations is not known for these correlations. Thus, it is of interest to check the accuracy of these correlations against the experimental data for upward inclined two-phase flows collected in this study and also with data available for different fluid combinations and pipe diameters from the literature. Based on the preliminary analysis done in Section 2.2, the correlations selected and listed in Table 2.1 will be scrutinized in this section against the present experimental data and also against the data set of the researchers reviewed in Section 2.1. The criteria used for evaluating the performance of these correlations is based on the percentage of data points predicted within ±20% and ±30% error bands. The maximum limit of the error band is taken as ±30% because it in the same order of magnitude as that of the maximum uncertainty calculated for the present experimental study. Also, the overall performance of these correlations for the entire data is analyzed using statistical parameters such as mean absolute error and standard deviation given by Equations (4.1) and (4.2), respectively.

$$\text{Absolute mean error} = \frac{1}{N}\sum_{j=1}^{N}\left|\varepsilon_j\right| \tag{4.1}$$

$$\text{Where } \left|\varepsilon_j\right| = \left|\frac{h_{TP,cal} - h_{TP,\exp}}{h_{TP,\exp}}\right|$$

$$\%\,\text{Std. deviation} = \sqrt{\frac{1}{N-1}\sum_{j=1}^{N}\left(\varepsilon_j - \bar{\varepsilon}\right)^2} \times 100 \tag{4.2}$$

The various wide range of parameters effecting the two-phase heat transfer coefficient are studied categorically in Section 4.2. So, in-order to facilitate the identification of best performing heat transfer correlations under the influence of these phenomena, the correlations in Table 2.1 are also applied on these data sets in the same order as seen in Section 4.2 except for Section 4.3.1, which

corresponds to the data sets discussed in both Sections 4.2.1 and 4.2.2. In this study any correlation considered to predict at-least 70% of the data points with an error band of ±30% was contemplated as a correlation with satisfactory performance and correlation predicting more than 90% of the data points is said to have done exceedingly well in predicting the two-phase flow heat transfer coefficient.

4.3.1 Effect of Flow Patterns and Pipe Orientation

As seen in Sections 4.2.1 and 4.2.2 for a 12.5mm stainless steel I.D. pipe with a length 101.6 cm in range of inclinations from 0^0 to $+90^0$, the heat transfer in two-phase flows is not only effected by the flow patterns but also by pipe inclination because these effects of flow patterns on h_{TP} are different in different inclination ranges, which are mainly grouped into horizontal and near horizontal inclinations ($0^0 \leq \theta \leq +30^0$), mid-range pipe inclinations ($+30^0 < \theta \leq +60^0$) and vertical and near vertical pipe inclinations ($+60^0 < \theta \leq +90^0$). The correlations given in Table 2.1 are analyzed for all flow patterns in these inclination ranges as seen in Tables 4.1, 4.2, 4.3 and 4.4. As mentioned earlier in Sections 4.2.1 and 4.2.2, the Re_{SL} and Re_{SG} for this data is varied between 1970 and 13200 and 290 and 19000, respectively. It can be seen from Table 4.1 that Tang and Ghajar (2007) was the best performing correlation for horizontal and near horizontal pipe inclinations, which was able to predict 262 out of 287 data points within an error limit of ±30%, in addition to smallest absolute mean error and standard deviation compared to any other correlation. This correlation was able to do exceedingly good for annular, stratified, slug and bubbly flows by predicting all these data points within the desired error band of ±30%. However, it should be noticed that this correlation under predicted the intermittent flow heat transfer coefficient consistently. For mid-range and vertical and near vertical orientations Shah (1981) proved to be the best performing correlation by predicting all the data points within an error band of ±30% and this is very closely followed by Tang and Ghajar (2007) for these pipe orientations, which was able to predict 163 out of 169 data points for mid-range pipe inclination and 152 out of 161 data points for vertical and near vertical pipe inclinations. It is

observed that the accuracy of the correlation of Tang and Ghajar (2007) was found to decrease for intermittent flows in these pipe orientations also, it under predicted the experimental data consistently. On the other hand despite of its best performance in mid-range and vertical and near vertical pipe inclinations, Shah (1981) was only able to predict 83% (238 out of 287) data points in the horizontal and near horizontal pipe orientations and this loss of accuracy is contributed by all flow patterns. These errors in prediction of Shah (1981) are all seen at low liquid flow rates ($Re_{SL} \leq$ 6600), where it over predicted the heat transfer coefficient. This is because of its inertia based correlation development for small hydraulic diameter tubes, which lacked sufficient pliability to incorporate the effects of buoyancy seen at these low liquid flow rates in this range of inclinations.

Table 4.1 Performance of non-boiling two phase heat transfer correlations for $0^o \leq \theta \leq +30^o$

Flow patterns	All flow patterns				Stratified		Slug		Intermittent		Bubbly		Annular	
No. of data points	287				5		79		144		7		52	
Correlations	(1)	(2)	(3)	(4)	(1)	(2)	(1)	(2)	(1)	(2)	(1)	(2)	(1)	(2)
Knott et al. (1959)	36	50	41	36	0	0	72	80	24	40	100	100	10	33
Dorresteijn (1970)	6	8	98	58	20	20	13	19	2	2	43	57	0	0
Martin and Sims (1971)	5	12	86	56	0	0	13	37	0	0	57	86	0	0
Khoze et al. (1976)	0	0	319	78	0	0	0	0	0	0	0	0	0	0
Aggour (1978)	4	9	109	70	0	0	10	24	0	0	57	86	0	0
Ravipudi and Godbold (1978)	11	17	107	82	0	0	34	49	0	2	71	100	0	0
Chu and Jones(1980)	0	0	144	92	0	0	0	0	0	0	0	0	0	0
Shah(1981)	72	83	17	21	0	0	81	86	69	83	100	100	71	85
Drucker et al. (1984)	32	46	32	20	40	60	72	96	19	33	100	100	0	0
Oshinowo et al. (1984)	0	0	539	163	0	0	0	0	0	0	0	0	0	0
Rezkallah and Sims (1987)	7	13	122	88	0	0	18	38	0	0	86	86	0	0
Kim and Ghajar (2006)	55	82	19	19	100	100	76	94	38	70	86	86	63	92
Tang and Ghajar (2007)	72	91	15	13	80	100	90	100	51	83	100	100	96	100

(1) % of data points predicted within ±20% error bands, (2) % of data points predicted within ±30% error bands, (3) % mean absolute error and (4) standard deviation.

Table 4.2 Performance of non-boiling two phase heat transfer correlations for $+30^{o} < \theta \leq +60^{o}$

Flow patterns	All flow patterns				Slug		Intermittent		Bubbly		Annular	
No. of data points	169				47		88		10		24	
Correlations	(1)	(2)	(3)	(4)	(1)	(2)	(1)	(2)	(1)	(2)	(1)	(2)
Knott et al. (1959)	80	90	14	17	98	100	76	89	100	100	54	71
Dorresteijn (1970)	18	27	51	31	49	72	0	1	80	100	0	0
Martin and Sims (1971)	27	44	40	29	68	87	5	24	100	100	0	8
Khoze et al. (1976)	0	0	238	35	0	0	0	0	0	0	0	0
Aggour (1978)	17	27	60	40	40	72	0	1	100	100	0	0
Ravipudi and Godbold (1978)	26	39	52	47	62	70	10	24	50	100	4	8
Chu and Jones(1980)	0	3	82	49	0	2	0	5	0	0	0	0
Shah(1981)	84	100	13	7	81	100	86	100	100	100	75	100
Drucker et al. (1984)	9	24	42	16	13	64	0	0	100	100	0	4
Oshinowo et al. (1984)	0	0	405	73	0	0	0	0	0	0	0	0
Rezkallah and Sims(1987)	25	32	63	52	68	81	0	6	100	100	0	4
Kim and Ghajar (2006)	29	48	28	16	70	98	0	10	100	100	25	67
Tang and Ghajar (2007)	64	96	16	10	94	100	35	93	100	100	96	100

(1) % of data points predicted within ±20% error bands, (2) % of data points predicted within ±30% error bands, (3) % mean absolute error and (4) standard deviation.

Some of the correlations are only developed with a limited range of applicability specifically aimed at extreme ranges of gas flow rates like Khoze et al.(1976), Chu and Jones (1980) and Oshinowo et al.(1984). Khoze et al. (1976) and Oshinowo et al. (1984) were unable to predict any data-points within a range of ±30% for this data set because the correlation of Oshinowo et al. (1984) was developed at very low gas and liquid superficial Reynolds numbers, while Khoze et al. (1976) was developed at very high gas flow rates and very low liquid Reynolds numbers as seen in Section 2.2. On the other hand Chu and Jones (1980) was only able to predict 24 out of 161 data points at vertical

and near vertical orientations especially in intermittent flow regime because of its development for high liquid inertial flows at Re_{SL} of 16000 to 112000. Apart from the above mentioned correlations all other correlations seem to perform pretty well in bubbly flow regime as seen in Table 4.4, while certain correlations like Kim and Ghajar (2006) were able to do reasonably well even in slug flow regime also. It should be observed that even Kim and Ghajar (2006) was equipped with a flow pattern factor to cover all the flow rates, its development was restricted to horizontal flows and hence led to a performance failure in inertia dominated intermittent and annular flows at vertical and near vertical flow regimes.

Table 4.3 Performance of non-boiling two phase heat transfer correlations for $+60^o < \theta \leq +90^o$

Flow patterns	All flow patterns				Slug		Intermittent		Bubbly		Annular	
No. of data points	161				28		87		16		30	
Correlations	(1)	(2)	(3)	(4)	(1)	(2)	(1)	(2)	(1)	(2)	(1)	(2)
Knott et al. (1959)	84	94	12	16	82	100	92	98	100	100	57	73
Dorresteijn (1970)	29	46	31	28	82	93	9	31	100	100	0	17
Martin and Sims (1971)	47	71	28	27	79	89	44	77	100	100	0	23
Khoze et al. (1976)	0	0	226	35	0	0	0	0	0	0	0	0
Aggour (1978)	25	34	43	44	68	75	6	20	100	100	0	0
Ravipudi and Godbold (1978)	35	53	39	43	64	71	38	55	31	100	0	7
Chu and Jones(1980)	0	15	68	47	0	4	0	18	0	38	0	3
Shah(1981)	43	100	19	7	29	100	39	100	88	100	43	100
Drucker et al. (1984)	6	17	46	15	7	43	0	0	44	94	0	0
Oshinowo et al. (1984)	0	0	376	71	0	0	0	0	0	0	0	0
Rezkallah and Sims(1987)	34	42	49	49	79	86	18	32	100	100	0	0
Kim and Ghajar (2006)	24	37	31	16	61	82	0	10	100	100	17	37
Tang and Ghajar (2007)	48	94	18	11	71	100	23	90	100	100	73	100

(1)% of data points predicted within ±20% error bands, (2) % of data points predicted within ±30% error bands, (3) % mean absolute error and (4) standard deviation.

Table 4.4 Performance of non-boiling two phase heat transfer correlations for $0^o \leq \theta \leq +90^o$

Flow patterns	All flow patterns				Slug		Intermittent		Bubbly		Annular		Stratified	
No. of data points	617				154		319		33		106		5	
Correlations	(1)	(2)	(3)	(4)	(1)	(2)	(1)	(2)	(1)	(2)	(1)	(2)	(1)	(2)
Knott et al. (1959)	61	72	26	33	82	90	57	69	100	100	33	53	0	0
Dorresteijn (1970)	15	23	68	55	36	49	3	10	82	91	0	5	20	20
Martin and Sims (1971)	22	36	59	51	42	62	13	28	91	97	0	8	0	0
Khoze et al. (1976)	0	0	272	73	0	0	0	0	0	0	0	0	0	0
Aggour (1978)	13	20	78	67	30	48	2	6	91	97	0	0	0	0
Ravipudi and Godbold (1978)	21	33	74	73	48	60	13	23	45	100	1	4	0	0
Chu and Jones (1980)	0	5	107	80	0	1	0	6	0	18	0	1	0	0
Shah(1981)	68	92	16	20	71	93	66	92	94	100	64	92	0	0
Drucker et al. (1984)	19	33	38	19	42	77	8	15	73	97	0	1	40	60
Oshinowo et al. (1984)	0	0	460	144	0	0	0	0	0	0	0	0	0	0
Rezkallah and Sims (1987)	19	26	87	78	44	60	5	10	97	97	0	1	0	0
Kim and Ghajar (2006)	40	61	24	19	71	93	17	37	97	97	42	71	100	100
Tang and Ghajar (2007)	64	94	16	12	88	100	39	87	100	100	90	100	80	100

(1)% of data points predicted within ±20% error bands, (2) % of data points predicted within ±30% error bands, (3) % mean absolute error and (4) standard deviation.

It should also be observed that only Kim and Ghajar (2006) and Tang and Ghajar (2007) were the only correlations noticed to perform reasonably well for stratified flow. However, it should be remembered that the total number of stratified flow data considered in this study are only five data points. It is also worth considering Knott et al. (1959) as a good performing correlation, which was

able to predict 72% of entire data set with in a ±30% error band despite performing poorly at horizontal and near horizontal inclinations by only predicting 50% of the data with in an error limit of ±30%. Many correlations that were able to predict h_{TP} satisfactorily for bubbly and slug flows, failed to predict the heat transfer coefficient in intermittent and annular flow regimes as seen in Table 4.4.

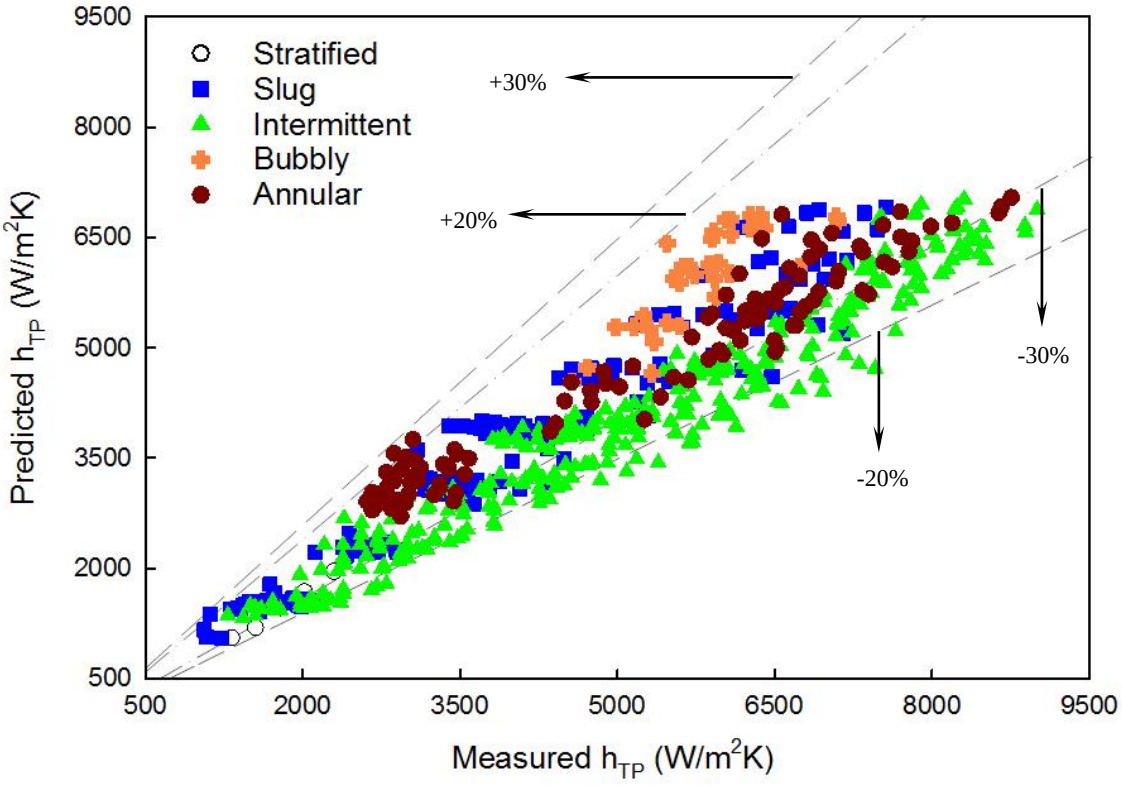

Figure 4.12 Performance of Tang and Ghajar (2007) correlation for all flow patterns

It is surveyed that Tang and Ghajar (2007) and Shah (1981) were the only correlations that were able to predict the heat transfer coefficient well in these flow patterns for the entire range, while Martin and Sims (1971) was able to perform well for these flow patterns only in vertical and near vertical pipe inclinations as shown in Table 4.3 and Knott et al. (1959) was able perform well in both mid-range and vertical and near vertical pipe inclinations as shown in Tables 4.2 and 4.3. On a whole for

this data set we can conclude that Tang and Ghajar (2007) was the best performing correlation as shown in Table 4.4. This correlation was able to predict 94% (577 out of 617) data points within an error band of ±30% and was followed by Shah (1981), which was able to predict 92% of this entire data set with in an error limit of ±30%. Also, Figures 4.12 and 4.13 show the performance of Tang and Ghajar (2007) for various flow patterns and various inclinations as discussed above.

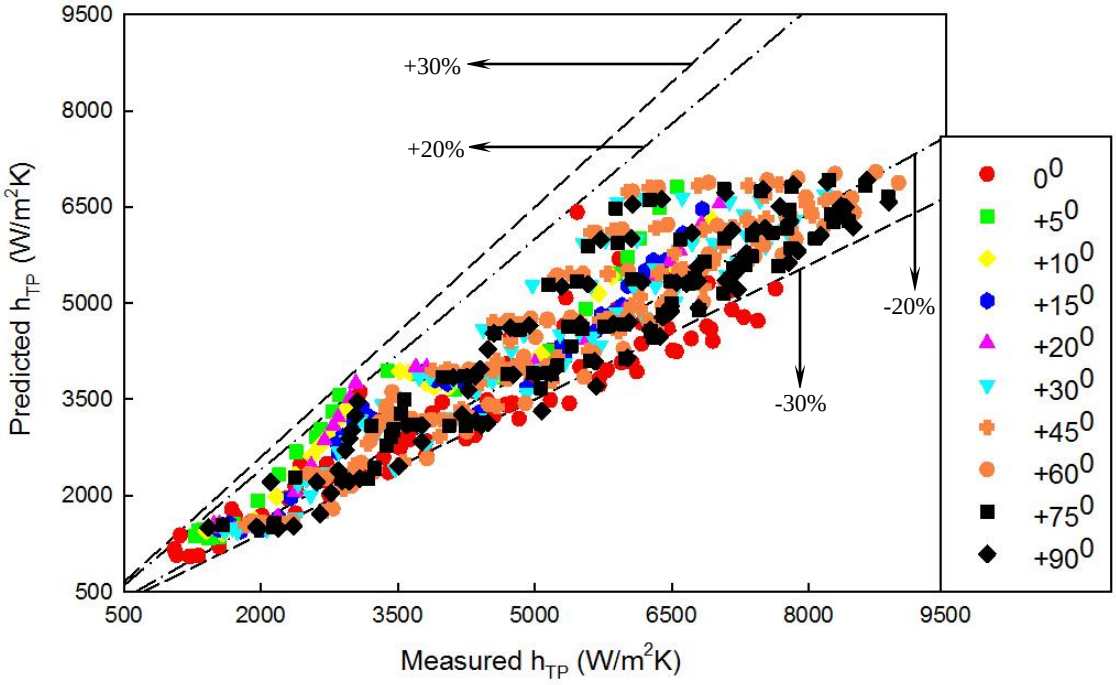

Figure 4.13 Performance of Tang and Ghajar (2007) correlation with respect to pipe orientations ($0^o \leq \theta \leq +90^o$)

4.3.2 Effect of Pipe Diameter

As seen in Section 4.2.3 the h_{TP} for two-phase flows is also greatly affected by the pipe diameter. Thus, it is of high importance for a good two phase heat transfer correlation to be able to incorporate this varying trend of heat transfer coefficient with respect to changing pipe diameter at various pipe orientations. In order to test the correlations given in Table 2.1 for these effects, analysis is done using the present data for 12.5mm diameter pipe, data of Sujumnog (1998), Vijay (1978) for 11.7mm diameter pipe, Tang and Ghajar (2007) for 27.9mm diameter pipe and Franca et al. (2008) for

18.6mm diameter pipe by using air-water as working fluid. This data considered for the present analysis consists of $+90^0$, $+0^0$ and $+5^0$ pipe orientations as shown in Tables 4.5 (a) and (b). The superficial Reynolds number ranges are also given in the Table 4.5 for each particular pipe diameter and pipe orientation, respectively.

Table 4.5(a): Performance of non-boiling two phase heat transfer correlations for various diameter pipes at different pipe inclinations.

Pipe Dimensions	D_i=11.7mm;l=610mm		D_i=12.5mm;l=889mm		D_i=12.5mm;l=889mm		D_i=27.9mm;l=2.64m	
No. of data points at a specified orientation	181@$+90^0$		86@$+90^0$		26@$+5^0$		184@$+5^0$	
Correlations	(1)	(2)	(1)	(2)	(1)	(2)	(1)	(2)
Knott et al. (1959)	82	92	81	92	8	12	21	28
Dorresteijn (1970)	17	30	27	49	0	0	4	7
Martin and Sims (1971)	70	88	44	67	0	0	1	8
Khoze et al. (1976)	0	0	0	0	0	0	0	0
Aggour (1978)	41	58	23	31	0	0	4	15
Ravipudi and Godbold (1978)	36	54	31	50	0	0	13	20
Chu and Jones(1980)	59	81	0	14	0	0	0	0
Shah(1981)	55	77	45	100	35	54	42	49
Drucker et al. (1984)	36	53	6	15	46	54	48	66
Oshinowo et al. (1984)	14	16	0	0	0	0	0	0
Rezkallah and Sims(1987)	53	61	31	40	0	0	4	9
Kim and Ghajar (2006)	42	65	24	37	69	88	66	83
Tang and Ghajar (2007)	56	80	49	91	96	100	92	97
Re_{SL} range	600-127000		1970-13200		1970-13200		700-26000	
Re_{SG} range	20-154000		290-19000		290-19000		700-48000	

(1)% of data points predicted within ±20% error bands, (2) % of data points predicted within ±30% error bands

Table 4.5(b): Performance of non-boiling two phase heat transfer correlations for various diameter pipes at horizontal inclination.

Pipe Dimensions	D_i=27.9mm;l=2.64m		D_i=12.5mm;l=889mm		D_i=18.7mm;l=5m	
No. of data points at a specified orientation	180@0^0		86@0^0		16@0^0	
Correlations	(1)	(2)	(1)	(2)	(1)	(2)
Knott et al. (1959)	3	10	36	52	6	31
Dorresteijn (1970)	0	0	8	8	0	0
Martin and Sims (1971)	0	0	3	9	0	0
Khoze et al. (1976)	0	0	0	0	0	0
Aggour (1978)	0	0	2	7	0	0
Ravipudi and Godbold (1978)	3	5	14	19	25	44
Chu and Jones(1980)	0	0	0	0	0	6
Shah(1981)	17	24	67	78	44	69
Drucker et al. (1984)	39	54	42	56	81	94
Oshinowo et al. (1984)	0	0	0	0	0	0
Rezkallah and Sims(1987)	0	1	7	10	0	0
Kim and Ghajar (2006)	53	71	60	90	69	88
Tang and Ghajar (2007)	68	83	43	73	50	88
Re_{SL} range	700-26000		1970-13200		8400-67000	
Re_{SG} range	700-48000		290-19000		2500-22000	

(1)% of data points predicted within ±20% error bands, (2) % of data points predicted within ±30% error bands

As seen in Section 4.3.1 the best performing correlation given by Tang and Ghajar (2007) for variable pipe inclinations and flow patterns is also able to do exceedingly well for variable pipe diameters at various pipe inclinations as shown in Table 4.5. However, Shah (1981), which have also been one of the best performing correlations for the data set given in Section 4.3.1, was only able to

predict 24% of data with in an error band of ±30% for the large diameter pipes as seen for D_i=27.9mm pipe in Table 4.5(b) at horizontal pipe inclination. It should also be noted that the accuracy of Shah (1981) was not only limited to vertical and near vertical orientation as seen in Section 4.3.1, but was also limited by phase flow rates. It was unable to predict the h_{TP} at very high gas flow rates like those seen in the case of 11.7mm diameter pipe, even though the data points correspond to vertical orientations. For this small pipe of 11.7mm diameter, it was able to predict 77% of the data with an error band of ±30% as seen in Table 4.5 due to the loss of accuracy at high gas flow rates. It can also be seen that many correlations like Knott et al. (1959), Shah (1981) and Martin and Sims (1971), which were predicting satisfactorily for low diameter pipes (D_i= 11.7mm, 12.5mm) at all orientations considered in this study and that of previous study from 0^0 to $+90^0$ as seen in Section 4.3.1, performed very poorly for increasing in the pipe diameters as seen in Table 4.5, for D_i= 18.6mm, 27.9mm. It should also be noted that even though Kim and Ghajar (2006) was able to include for the effects of changing pipe diameter on h_{TP}, its performance is only limited to horizontal and near horizontal inclinations (0^0 and $+5^0$ for the present data set) as seen in Table 4.5. Thus, leaving Ghajar and Tang (2007) as the only capable correlation for predicting h_{TP} irrespective of pipe diameter.

4.3.3 Effect of Fluid Properties

As seen in Section 4.2.4, the h_{TP} for two phase flows is effected by the fluid combinations mainly because of the variation in liquid viscosity, liquid thermal conductivity and gas density. For the purpose of analyzing the effect of varying fluid combinations on the performance of correlations, data of Sujumnong (1998), Aggour (1978), Rezkallah and Sims (1987) and Vijay (1978) measured in 11.7 mm diameter pipe at vertical orientation ($+90^0$) was used. The physical and thermal properties of various fluid combinations corresponding to different sources are given in Table 4.6. It should be noted that air-glycerine (59%) +water (41%) and air-silicone are used to see the effect of varying viscosity on correlation performance with respect to air-water and in a

similar way, feron12-water and helium-water are used to see the effect of varying gas density on correlational performance with respect to air-water as shown in Table 4.7.

Table 4.6 Summary of physical and thermal properties for data sets used to assess the correlational performance

Source	Fluid Combination	k_L	k_G	$\mu_{L\ X\ 10^3}$	$\mu_{G\ X\ 10^3}$	ρ_L	ρ_G
Aggour(1978)	Helium-water	0.606	0.15	0.840-1.01	1.99	999	0.162-0.167
	Freon12-water	0.61	0.0101	0.821-0.911	1.09	998	5.12
Vijay (1978)	Air-water	0.602	0.0258	0.853-1.12	1.82	999	1.18-1.22
Rezkallah (1987)	Air-Silicone	0.117	0.0261	4.54-5.02	1.84	917	1.18-1.19
Sujumnong (1998)	Air-Water	0.609	0.0262	0.772-1.01	1.84	998	1.18-4.04
	Air-glycerin(59%) +water(41%)	0.385	0.0259	8.50-11.1	1.82	1150	1.31-3.64

Before looking into the results, it should be noticed that all these data sets correspond to a small diameter pipe(11.7mm) at vertical orientations (+90), which favors inertial flow conditions and correlations that were specified to include these factors tend to perform well for these fluid combinations accordingly. So, it should be noticed that despite failing to predict the effects of pipe diameter and pipe orientation on heat transfer coefficient, certain correlations like Knott et al. (1959) and Shah (1981) were able to perform well for all the fluid combinations used, except for flows with high gas density corresponding to feron12-water as shown in Table 4.7. It was also observed that Ghajar and Tang (2007) was able to predict h_{TP} satisfactorily for fluid combinations with varying liquid viscosity and for fluid combinations with high gas density corresponding to feron12-water but was only able to predict only 50% of the data points with in an error band of ±30% for fluid combination of helium-water, which corresponds to very low gas density as seen in Table 4.7. This might be because of ignoring the influence of the surface tension and the contact angle of each phase on the effective wetted perimeter as mentioned in Section 2.2. However it should be noted that the analysis presented in this section corresponds to limited

number of data points in a small pipe diameter taken at a single orientation and hence more analysis is required to verify these observation in a wider spectrum.

Table 4.7 Performance of non-boiling two phase heat transfer correlations for various fluid combination at vertical inclination in 11.7mm pipe

Fluid Combination	Air-Glycerin+Water		Air-Silicone		Air-Water		Freon12-Water		Helium-Water	
No. of data points	51		56		181		44		50	
Correlations	(1)	(2)	(1)	(2)	(1)	(2)	(1)	(2)	(1)	(2)
Knott et al. (1959)	84	100	80	89	82	92	36	57	82	90
Dorresteijn (1970)	24	41	34	52	17	30	57	70	16	24
Martin and Sims (1971)	39	57	48	61	70	88	82	91	40	74
Khoze et al. (1976)	0	0	0	0	0	0	0	0	6	8
Aggour (1978)	0	0	0	0	41	58	77	82	28	34
Ravipudi and Godbold (1978)	63	69	26	41	36	54	23	55	34	44
Chu and Jones (1980)	0	0	21	38	59	81	80	86	48	60
Shah(1981)	53	76	73	91	55	77	34	39	44	78
Drucker et al. (1984)	49	53	86	98	36	53	20	30	26	30
Oshinowo et al. (1984)	0	0	0	4	14	16	20	25	6	6
Rezkallah and Sims (1987)	0	0	55	64	53	61	73	84	30	40
Kim and Ghajar (2006)	41	55	57	88	42	65	30	43	20	50
Tang and Ghajar (2007)	29	67	48	86	56	80	34	75	22	50

(1)% of data points predicted within ±20% error bands, (2) % of data points predicted within ±30% error bands

CHAPTER V

CONCLUSIONS AND RECOMMENDATIONS

In the present study major parameters that influence the two-phase two-component heat transfer in upward flows were determined to be pipe inclination, phase flow rates, pipe diameter and fluid combination. A systematic investigation was done to understand the effect of pipe orientation, phase flow rates, pipe diameter and fluid combinations on two-phase heat transfer coefficient (h_{TP}) and two-phase flow patterns. In addition to these, this study was also able to identify the most widely used two-phase heat transfer correlations and asses the performance of these correlations for varying pipe orientations, phase flow rates, pipe diameter and fluid combinations. A total of 617 data points were collected at $0^0 \leq \theta \leq +90^0$ inclination ranges in 12.5 mm I.D. polycarbonate stainless steel pipe using air-water fluid combination, beside the additional data from the literature as mentioned in Section 2.1 to analyze for the above mentioned effects. Following is a brief summary of the present study, as well as recommendations for possible future study.

5.1 Conclusion of Results

Flow Patterns and Flow Pattern Maps

It is identified that upward flow exhibits slug, bubbly, intermittent and annular flow patterns with an exception of stratified flow pattern that was observed at horizontal pipe inclination only. It was noted that phase flow rates significantly affect the two-phase flow pattern and was concluded

that with the increase in gas flow rate the buoyancy driven flow patterns (slug flow pattern and bubbly flow patterns) tend to shift towards inertial flow patterns (intermittent and annular). An increase in liquid flow rates was found to enable a homogeneous flow structure with slug flow pattern shifting to bubbly flow pattern at lower gas flow rates.

It is observed that buoyancy driven flow patterns are more sensitive to pipe orientation than inertial driven flow patterns and also an increased tendency to attain inertial driven flow patterns was noted with an increase in pipe orientation. A change in the physical structure of the flow pattern was also identified with a tendency to attain axisymmetric flow structure with respect to increasing pipe orientations.

Heat Transfer in Two-phase Two-Component Flows

It was observed that at low liquid flow rates in slug flow regime the h_{TP} is relatively insensitive to increase in gas flow rates particular for horizontal and mid-range pipe inclinations. At vertical and near vertical pipe inclinations in the slug flow regime an increase in h_{TP} was observed with an increase in gas flow rate. It was shown that these effects are due to the change in physical structure of the flow pattern and also by partial downward flowing liquid film in slug flows.

At low gas flow rates with increase in liquid flow rate the increase in h_{TP} tends to decrease due to change of flow structure from slug to bubbly for all pipe inclinations. However in these high liquid flow rates corresponding to bubbly flow regime the h_{TP} tends to increase consistently for all pipe inclinations with respect to increasing gas flow rate. In intermittent and annular flow patterns with an increase in gas flow rates at all liquid flow rates, the h_{TP} tends to increase with an increasing slope because of the turbulent nature in the flows owing to the formation of a continuous liquid film in contact with the wall except at low liquid flow rates in mid-range and vertical and near vertical pipe inclinations due to liquid holdup.

It was observed that the h_{TP} tends to increase with respect to increasing pipe orientation and tends to attain a maximum at around $+60^0$ to $+75^0$ depending on the liquid flow rates. This variation in h_{TP} with respect to pipe inclination is due to the interaction between the gravitational and buoyancy forces on the two-phase flows. It was observed that at low liquid flow rates ($Re_{SL} \leq 3300$) the maximum h_{TP} is achieved at $+75^0$ and then the h_{TP} decreases till $+90^0$ due to the liquid holdup induced by gravity. At medium and high liquid flow rates ($Re_{SL} > 3300$) the maximum h_{TP} was found to occur at $+60^0$ and then the h_{TP} is found to stay constant with respect to increasing pipe inclination because of the reduction in liquid hold-up caused by the high liquid flow rates promoting a more homogeneous flow structure.

It was observed that the h_{TP} in small diameter pipes is greater than the h_{TP} measured in large diameter pipes and this effect of pipe diameter is significantly large in inertia driven flow patterns compared to buoyancy driven flow patterns. It is also observed that the increase in pipe diameter delays the transmission from buoyancy driven flow patterns to inertia driven flow patterns. It is also observed that the liquid properties like thermal conductivity, viscosity and density greatly influence the h_{TP}, particularly at higher flow rates.

Analysis of Heat Transfer Correlations Performance

It was observed that many of the correlations were able to perform well for bubbly flow patterns and a few correlations like Knott et al. (1959) and Kim and Ghajar (2006) were able to also perform satisfactorily for slug flows also for 12.5 mm pipe. It was concluded that Tang and Ghajar (2007) and Shah (1981) heat transfer correlations were able to perform exceedingly well for 12.5 mm pipe by predicting 94% and 92% of data points with in an error limit of ±30%, respectively.

It was observed that for larger diameter pipes the accuracy of Shah (1981) heat transfer correlation dropped drastically at all tested orientations. However, Tang and Ghajar (2007) proved to perform well for the tested pipe diameters at all pipe inclinations. It was also concluded that Tang and Ghajar (2007) was able to do exceedingly well for change in liquid phase properties and was able to perform satisfactorily for change in gas phase properties.

5.2 Future Recommendations

1) Incorporate the experimental results and analysis of John et al. (2015) for downward pipe orientations ($-90^0 \leq \theta \leq 0^0$) and perform an overall analysis to cover the full range of pipe orientations ($-90^0 \leq \theta \leq +90^0$) for the present experimental setup.

2) Test the heat transfer correlations for variable fluid properties at larger diameter pipes also, to see the best performing correlations. Test the heat transfer correlations for variable pipe diameters at both upward and downward inclinations in addition to the standard horizontal and vertical pipe inclinations.

REFERENCES

Aggour, M. A. (1978). Hydrodynamics and Heat Transfer in Two-Phase Two-Component Flow. (Ph.D. Dissertation), University of Manitoba, Canada. Aggour, M. A. (1978). Hydrodynamics and Heat Transfer in Two-Phase Two-Component Flow. (Ph.D. Dissertation), University of Manitoba, Canada.

Barnea, D., Shoham, O. & Taitel, Y. (1982). Flow Pattern Transition for Downward Inclined Two Phase Flow: Horizontal to Vertical, *Chemical Engineering Science*, Vol. 37, pp. 735-740.

Bendiksen, K.H.(1984). An Experimental Investigation of the Motion of Long Bubbles in Inclined Tubes, International Journal of Multiphase Flow, Vol. 10, pp. 467-483.

Bhagwat, S. M., Mollamahmutoglu, M., & Ghajar, A. J. (2012). Experimental Investigation and Empirical Analysis of Non-Boiling Gas-Liquid Two Phase Heat Transfer in Vertical Downward Pipe Orientation. *Proceedings of ASME 2012 Summer Heat Transfer Conference (HT2012)*, Puerto Rico, July 8-12.

Bhagwat, S. M. (2015). Experimental Measurements and Modeling of Void Fraction and Pressure Drop in Upward and Downward Inclined Non-Boiling Gas-Liquid Two Phase Flow. (Ph.D.), Oklahoma State University, Stillwater, Oklahoma.

Carey, V. P. (1992). *Liquid-Vapor Phase-Change Phenomena: An Introduction to the Thermophysics of Vaporization and Condensation Process in Heat Transfer Equipment*, Taylor & Francis, Bristol, UK.

Celata, G. P., Chiaradia, A., Cumo, M., & D'Annibale, F. (1999). Heat Transfer Enhancement by Air Injection in Upward Heated Mixed-Convection Flow of Water, *International Journal of Multiphase Flow*, vol. 25, pp. 1033–1052.

Chisholm, D. (1973). Void Fraction During Two-Phase Flow. *J. Mechanical Engineering Science*, Vol. 15, pp. 235-236.

Chu, Y. C., & Jones, B. G. (1980). Convective Heat Transfer Coefficient Studies in Upward and Downward Vertical Two-Phase Non-Boiling Flows. *AIChE., Vol. 7*, pp. 79-90.

Cook, W. L. (2008). An Experimental Apparatus for Measurement of Pressure Drop, Void Fraction, and Non-Boiling Two-Phase Heat Transfer and Flow Visualization in Pipes for All Inclinations. (MS), Oklahoma State University, Stillwater.

Crawford, T. J. (1983). Analysis of Steady State and Transient Two Phase Flows in Downwardly Inclined Lines. (Ph.D), Drexel University.

Dittus, F.W. & Boelter, L.M.K (1930). Heat Transfer Inautomobile Radiators of The Tubular Type. *University of California Publications in Engineering*, Vol. 2, pp. 443-461.

Dorresteijn, W. R. (1970). Experimental Study of Heat Transfer in Upward and Downward Two Phase Flow of Air and Oil through 700 M Tubes. *Proccedings of the 4th International Heat Transfer Conference*, Vol. 5, B5.9, Paris & Versailles, France.

Drucker, M. I., Dhir, V. K., & Duffey, R. B. (1984). Two Phase Heat Transfer for Flow in Tubes and over Rod Bundles with Blockages. *Trans. of ASME, J. of Heat Transfer*, Vol. 106, no. 4, pp. 856-864.

Franca, F. A., Bannwart, A. C., Camargo, R. M. T., & Gonçalves, M. A. L. (2008). Mechanistic Modeling of the Convective Heat Transfer Coefficient in Gas-Liquid Intermittent Flows, Heat Transfer Engineering, Vol. 29, no. 12, pp. 984–998.

Ghajar, A. J., & Tam, L. M. (1994). Heat Transfer Measurements and Correlations in the Transition Region for a Circular Tube with Three Different Inlet Configurations, Experimental Thermal and Fluid Science, Vol. 8, pp. 79-90.

Ghajar, A.J. & Kim, J. (2005), "A Non-Boiling Two-Phase Heat Transfer Correlation for Different Flow Patterns and Pipe Inclination Angles," Proceedings of the 2005 ASME Summer Heat Transfer Conference, July 17-22, SanFrancisco, CA.

Ghajar, A. J., & Kim, J. (2006). *Calculation of Local inside-Wall Convective Heat Transfer Parameters from Measurements of the Local Outside-Wall Temperatures Along an Electrically Heated Circular Tube, Heat Transfer Calculations*. NewYork, NY: Mc-Graw-Hill.

Godbole P.V., Tang C.C., & A.J. Ghajar (2011). Comparison of void fraction correlations for different flow patterns in upward vertical two phase flow. *Heat Transfer Engineering*, Vol. 32, no. 10, pp. 843–860.

Groothuis, H., & Hendal, W.B (1959). Heat Transfer in Two-phase Flow, Chem. Eng. Sci., Vol. 11, pp. 212-220.

Hossainy, T. A. (2014). Non-Boiling Heat Transfer in Horizontal and near Horizontal Downward Inclined Gas-Liquid Two Phase Flow. (MSc.), Oklahoma State University, Stillwater, Oklahoma.

Hossainy, T. A., Bhagwat, S. M., & Ghajar, A. J. (2014). Non-Boiling Heat Transfer in Horizontal and near Horizontal Downward Inclined Gas-Liquid Two Phase Flow. *10th International Conference on Heat Transfer, Fluid Mechanics and Thermodynamics*, Orlando, Florida.

Johnson, H. A., & Abou-Sabe, A. H. (1952). Heat Transfer and Pressure Drop for Turbulent Flow of Air-Water Mixture in a Horizontal Pipe. Trans. ASME, Vol. 50, no. 9,pp. 47–51.

John, T. J., Bhagwat, S. M., & Ghajar, A. J. (2015). Heat Transfer Measurement and Correlations Assessment for Downward Inclined Gas-Liquid Two Phase Flow. *Proceedings of the 1st Thermal and Fluid Engineering Summer Conference*, New York City, USA, August 9-12.

Kalapatapu, S.,Oyewole, A.L., Bhagwat, S.M. & Ghajar, A.J. (2014). "Non-Boiling Heat Transfer in Horizontal and near Horizontal Upwnward Inclined Gas-Liquid Two Phase Flow," Proceedings of the 10th International Conference on Heat Transfer, Fluid Mechanics and Thermodynamics, Orlando, Florida.

Khoze, A. N., Dunayev, S. V., & Sparin, V. A. (1976). Heat and Mass Transfer in Rising Two-Phase Flows in Rectangular Channels. *Heat Transfer - Soviet Research,* Vol. 8, no. 3,pp. 87-90.

Kim, J., & Ghajar, A. J. (2006). A General Heat Transfer Correlation for Non-Boiling Gas-Liquid Flow with Different Flow Patterns in Horizontal Pipes. *Int. J. Multiphase Flow,* VOl. 32, pp. 447–465.

Kline, S. J., & McClintock, F. A. (1953). Describing Uncertainties in Single Sample Experiments. *Mechanical Engineering,* Vol. 1, pp. 3-8.

Knott, R. F., Anderson, R. N., Acrivos, A., & Petersen, E. E. (1959). An Experimental Study of Heat Transfer to Nitrogen-Oil Mixtures. *Industrial and Engineering Chemistry,* Vol. 51, no. 11, pp. 1369-1372.

Korivi, R. N. K, Bhagwat, S. M., & Ghajar, A. J. (2015). Heat Transfer Measurement and Correlations Assessment for Upward Inclined Gas-Liquid Two Phase Flow. *Proceedings of the 1st Thermal and Fluid Engineering Summer Conference*, New York City, USA, August 9-12.

McClaflin, G. G. & Whitfill, D. L. (1984). Control of Paraffin Deposition in Production Operations, *Journal of Petroleum Technology*, vol. 36, no. 12, pp. 1965–1970.

Martin, B. W., & Sims, G. E. (1971). Forced Convection Heat Transfer to Water with Air Injection in a Rectangular Duct. *I&EC Fundamentals,* Vol. 14,pp. 1115–1134.

Mollamahmutoglu, M. (2012). Study of Isothermal Pressure Drop and Non-Boiling Heat Transfer in Vertical Downward Two Phase Flow. (M.S.), Oklahoma State University, Stillwater, Oklahoma.

Oshinowo, O., Betts, R. C., & Charles, M. E. (1984). Heat Transfer in Co-Current Vertical Two-Phase Flow. *Canadian Journal of Chemical Engineering,* Vol. 62, pp. 194-198.

Ravipudi, S. R., & Godbold, T. M. (1978). The Effect of Mass Transfer on Heat Transfer Rates for Two-Phase Flow in Vertical Pipe. *Proceedings of the 6th International Heat Transfer Conference*, Vol. 1, pp. 505–510, Toronto, Canada.

Rezkallah, K. S. (1987). Heat Transfer and Hydrodynamics in Two-Phase Two-Component Flow in a Vertical Tube, Ph.D. Thesis, University of Manitoba, Winnipeg, Manitoba, Canada.

Rezkallah, K. S., & Sims, G. E. (1987). An Examination of Correlations of Mean Heat Transfer Coefficients in Twophase and Two-Component Flow in Vertical Tubes. *AIChE Symp. Series*, Vol. 83, pp. 109-114.

Shah, M. M. (1981). Generalized Prediciton of Heat Transfer During Two-Component Gas-Liquid Flow in Tubes and Other Channels. *AIChE Symp. Series*, Vol. 77, pp. 140-151.

Sieder, E. N., & Tate, G. E. (1936). Heat Transfer and Pressure Drop of Liquids in Tubes. *Industrial and Engineering Chemistry*, Vol. 28, pp. 1429-1435.

Singh, P., Venkatesan, R., Fogler, H. S., & Nagarajan, N. (2000). Formation and Aging of Incipient Thin Film Wax-Oil Gels, *AIChE Journal*, vol. 46, no. 5, pp. 1059–1074.

Spedding, P.L. & Chen, J.J.J. (1984), "Holding in Two Phase Flow," International Journal of Multiphase Flow, Vol. 10, no. 3, pp. 307-339.

Spedding, P.L., Woods, G.S., Raghunathan, S.R., & Watterson, J.k., (2000). Flow Pattern, Holdup and Pressure Drop in Vertical and Near vertical Two and Three Phase Upflow. Institution of Chemical Engineers, Trans. of IChemE 78, pp. 404–418.

Sujumnong, M. (1998). Heat Transfer, Pressure Drop and Void Fraction in Two-Phase, Two Component Flow in a Vertical Tube, Ph.D. Thesis, University of Manitoba, Winnipeg, Manitoba, Canada.

Taitel, & Dukler, A.E., 1976. A Model for Predicting Flow Regime Transitions in Horizontal and Near Horizontal Gas-Liquid Flow. AIChE 22, 47–55.

Tang, C. C. (2011). A Study of Heat Transfer in Non-Boiling Two-Phase Gas-Liquid Flow in Pipes for Horizontal, Slightly Inclined, and Vertical Orientations. (Ph.D.), Oklahoma State University, Stillwater, Oklahoma.

Tang, C. C., & Ghajar, A. J. (2007). Validation of a General Heat Transfer Correlation for Non-Boiling Two-Phase Flow with Different Flow Patterns and Pipe Inclination Angles. *Proceedings of the 2005 ASME-JSME Thermal Engineering Heat Transfer Connference*, Vancouver, Canada, July 8-12.

Vijay, M. M. (1978). A Study of Heat Transfer in Two-phase Two-componet Flow in a Vertical Tube. (Ph.D.), University of Manitoba, Winnipeg, Manitoba.

APPENDIX A

UNCERTAINTY ANALYSIS

The uncertainty associated with the two-phase and single-phase flows is calculated from the method proposed by Kline and McClintok (1953) and the uncertainty associated with present flow variables was given in Section 3.4 of Experimental setup. A scheme used to perform the uncertainty analysis was given in this section. According to Kline and McClintock (1953) firstly, the uncertainty of the independent variable in the heat transfer coefficient equation are calculated separately and then these individual uncertainties are replaced in the formula to calculate the total uncertainty of the heat transfer coefficient. Let a function R be dependent on several independent variables as shown in Equation (A.1), then the uncertainty associated with the variable R can be obtained by using Equation (A.2).

$$R = f(x_1, x_2, x_3 \ldots\ldots\ldots\ldots\ldots x_n) \tag{A.1}$$

$$w_R = \pm[(\frac{dR}{dx_1}w_1)^2 + (\frac{dR}{dx_2}w_2)^2 + (\frac{dR}{dx_3}w_3)^2 + \quad \ldots\ldots\ldots \quad + (\frac{dR}{dx_n}w_n)^2\ ]^{\frac{1}{2}} \tag{A.2}$$

The heat transfer coefficient equation is given by

$$h = \frac{\dot{q}''}{\bar{T}_{wi} - \bar{T}_b} = \frac{\dot{q}''}{\Delta T} \tag{A.3}$$

So, h is a function of $\dot{q}''$ and ΔT. Hence, in-order to determine the uncertainty associated with h. It is necessary to determine the uncertainty associated with $\dot{q}''$ and ΔT as show below.

$$w_h = \left[\left(\frac{\partial h}{\partial \dot{q}''} w_{\dot{q}''} \right)^2 + \left(\frac{\partial h}{\partial \Delta T} w_{\Delta T} \right)^2 \right]^{\frac{1}{2}} \tag{A.4}$$

$$w_h = \left[\left(\frac{1}{\Delta T} w_{\dot{q}''} \right)^2 + \left(\frac{-\dot{q}''}{\Delta T} w_{\Delta T} \right)^2 \right]^{\frac{1}{2}} \tag{A.5}$$

the uncertainty associated with ΔT can be found by adding the uncertainties associated with $\bar{T}_{wi}(average\ inside\ wall\ surface\ temperature)$ and $\bar{T}_b$(average bulk temperature of the fluid mixture).

From the setup the outside wall temperature at all four thermocouples for each station are procured and averaged to obtain the average wall outside surface temperature at each station.

$$\bar{T}_{wo-n} = \frac{T_{wo-1}+T_{wo-2}+T_{wo-3}+T_{wo-4}}{4} \tag{A.6}$$

There are seven thermocouple stations in the setup. So, the average outside wall surface temperature for the whole setup is calculated by

$$\bar{T}_{wo} = \frac{\bar{T}_{wo-1}+\bar{T}_{wo-2}+\bar{T}_{wo-3}+\bar{T}_{wo-4}+\bar{T}_{wo-5}+\bar{T}_{wo-6}+\bar{T}_{wo-7}}{7} \tag{A.7}$$

Hence, the average wall outside surface temperature uncertainty is $\pm 0.5^0$C because the uncertainty associated with each thermocouple temperature measurement is $\pm 0.5^0$C.

Thermal resistance of the setup is a function of outer diameter (D_0), inner diameter (D_i), thermal conductivity (k) and heat transfer length (l) as shown in Equation (A.8). So, the uncertainty in thermal resistance is given by Equation (A.9). The uncertainties associated with the outer pipe diameter, inner pipe diameter, thermal conductivity, heat transfer length are standard and are given in Table 3.1 and Table 3.4 for two-phase and single-phase flows, respectively. From this the uncertainty value associated with the thermal resistance is determined to be ±0.51%.

$$R_t = \frac{\ln\left(D_o / D_i\right)}{2\pi kl} \tag{A.8}$$

$$w_{R_t} = \left[\left(\frac{1}{2\pi D_o kl} w_{D_o} \right)^2 + \left(\frac{-1}{2\pi D_i kl} w_{D_i} \right)^2 + \left(\frac{-\ln\left(D_o / D_i\right)}{2\pi k^2 l} w_k \right)^2 + \left(\frac{-\ln\left(D_o / D_i\right)}{2\pi l^2 k} w_l \right)^2 \right]^{\frac{1}{2}} \tag{A.9}$$

The heat transfer rate is calculated from the voltage and current input of the welder and is given by Equation (A.10). The associated uncertainty was determined by Equation (A.11).

$$\dot{q} = V_D I \tag{A.10}$$

$$w_{\dot{q}} = \left[\left(I w_{V_D} \right)^2 + \left(V_D w_I \right)^2 \right]^{\frac{1}{2}} \tag{A.11}$$

While, this uncertainty regarding heat transfer rate is calculated by using the equation for heat input from the welder which takes in account the manufacturer prescribed uncertainties for the voltage (V_D) and current (I). However, there is also heat loss due to the surroundings from the setup and heat storage in the setup. This amount of heat loss can be calculated from the difference between the heat input rate from the welder and heat transfer rate calculated by using the enthalpy equation to the flow which is also called heat balance error and this heat balance error should be added with the uncertainty obtained by using Eq. (A.11) to obtain the total uncertainty of heat transfer rate.

The average wall inside surface temperature is given by Equation (A.12) as a function of the wall outside surface temperature, thermal resistance and heat transfer rate. So, likewise the uncertainty associated with it is given by Equation (A.13) as a function of uncertainties of wall outside surface temperature, thermal resistance and heat transfer rate.

$$\bar{T}_{wi} = \dot{q}R_t + \bar{T}_{wo} \tag{A.12}$$

$$w_{\bar{T}_{wi}} = \left[\left(R_t w_{\dot{q}} \right)^2 + \left(\dot{q} w_{R_t} \right)^2 + \left(w_{\bar{T}_{wo}} \right)^2 \right]^{\frac{1}{2}} \tag{A.13}$$

Using the Equations (A.7), (A.9) and (A.11) in addition to the uncertainty of independent variables, Equation (A.13) is solved to find the uncertainty associated with the average wall inside surface temperature and hence the uncertainty associated with ΔT.

The heat flux is obtained from the total heat transfer rate and circumferential area as given by Equation (A.14) and uncertainty associated with it is given by Equation (A.15).

$$\dot{q}'' = \frac{V_D I}{\pi D_i l} \tag{A.14}$$

$$w_{\dot{q}''} = \left[\left(\frac{I}{\pi D_i l} w_{V_D} \right)^2 + \left(\frac{V_D}{\pi D_i l} w_I \right)^2 + \left(\frac{-V_D I}{\pi D^2{}_i l} w_{D_i} \right)^2 + \left(\frac{-V_D I}{\pi D_i l^2} w_l \right)^2 \right]^{\frac{1}{2}} \tag{A.15}$$

The uncertainty in voltage drop, current, inner diameter and heat transfer length are all standard values and can be found in Table 3.1 and Table 3.4 for two-phase and single-phase flows, respectively.

Therefore, by substituting Equation (A.13) and Equation (A.15) into Equation (A.5) the total uncertainty of the heat transfer coefficient (h) was obtained.

VITA

Korivi Ranga Nanda Kishore

Candidate for the Degree of

Master of Science

Thesis: HYDRODYNAMICS AND HEAT TRANSFER IN UPWARD INCLINED GAS-LIQUID TWO-PHASE TWO-COMPONENT FLOWS

Major Field: Mechanical and Aerospace Engineering

Biographical: Born and raised in Andhra Pradesh, India.

Education:

Completed the requirements for the Master of Science in Mechanical Engineering at Oklahoma State University, Stillwater, Oklahoma in December 2015.

Completed the requirements for the Bachelor of Technology in Mechanical Engineering at Jawaharlal Nehru Technological University, Kakinada, India in May 2013.

Experience:

Graduate Teaching Assistant January 2014-December 2015
Mechanical and Aerospace Engineering Dept., Oklahoma State University, OK

1. Organize the lab equipment and instruct the students on procedure in Measurements and Instrumentation laboratory in addition to Grading lab reports and lab exams.
2. Assist students of Senior Design in completions of projects and preparation of reports.
3. Grad and assist students of Energy conversion in homework's and projects.